Acta Appl Math (2015) 137:123–157
DOI 10.1007/s10440-014-9993-x

Problems on Time-Varying Domains: Formulation, Dynamics, and Challenges

E. Knobloch · R. Krechetnikov

Received: 8 July 2014 / Accepted: 3 November 2014 / Published online: 9 December 2014

Abstract The purpose of this article is to introduce the reader to phenomena on time-varying spatial domains and to highlight the differences from their counterpart on time-fixed domains. We begin by discussing the origin of this class of problems in various physical systems and applications, and then provide a general formulation from both Lagrangian and Eulerian viewpoints with the goal of identifying a set of basic principles necessary for understanding new effects on time-dependent domains. The distinctive features of the dynamics are illustrated with the help of two representative examples discussed in detail: (1) propagation of longitudinal waves in a stretching rod, and (2) Eckhaus instability of a stretching spatially periodic pattern. In view of the evolving character of the subject, we conclude with a number of open questions.

Keywords Time-dependent domains · Pattern formation · Eckhaus instability

Mathematics Subject Classification 34Dxx · 70K50 · 65Mxx · 35R35 · 37Lxx · 37Kxx

1 Introduction: Objectives and Outline

The goal of this paper is to introduce the reader to the vast subject of phenomena on time-dependent spatial domains by highlighting the key foundational contributions. We begin in Sect. 2 with a discussion of a number of representative physical examples from various fields, which will help us develop basic intuition about the behavior exhibited by such systems, and then in Sect. 3 introduce the key mathematical elements uniting these seemingly different physical examples, thereby providing basic theoretical foundation for treating problems on time-dependent domains. Section 4 discusses in detail two illustrative

E. Knobloch
Department of Physics, University of California, Berkeley, CA 94720, USA
e-mail: knobloch@berkeley.edu

R. Krechetnikov (✉)
Department of Mathematics, University of Alberta, Edmonton, AB T6G 2G1, Canada
e-mail: krechet@ualberta.ca

problems—propagation of longitudinal waves in a stretching rod and Eckhaus instability of a stretching spatially periodic pattern—which will deepen understanding of the key new effects observed in problems on time-dependent domains.

While the discussion of concrete physical phenomena is postponed to the main body of the paper, it is worthwhile to introduce an overview of the problems at hand and some classifications. Although time-dependence of the spatial domain implies that the problem is distributed in space and thus infinite-dimensional, there are some systems where a finite-dimensional description suffices to capture the physics. This is the case for some problems in fluid-structure interaction (Sect. 2.4) such as flutter, particles in a time-dependent potential well (Sect. 2.6), and control theory (Sect. 2.3). However, most of the systems studied, ranging from fluid dynamics (Sect. 2.1) and astrophysics (Sect. 2.2) to pattern formation in biology (Sect. 2.7) and solidification (Sect. 2.8), are indeed infinite-dimensional.

The standard classification of partial differential equations (PDEs) into parabolic, hyperbolic, and elliptic, offers an alternative, but unifying, view of these problems [118]. For example, parabolic PDEs include reaction-diffusion systems, solidification and crystal growth, as well as Stefan and Skorokhod problems. Hyperbolic PDEs include wave propagation, fluid-structure interaction, extensible beam dynamics, cavity resonators, and many problems in fluid dynamics. In contrast, elliptic PDEs are mostly irrelevant since we are concerned with time evolution. At the nonlinear level, among other evolution systems studied on time-dependent domains are the Navier-Stokes equations [39], Korteweg-de Vries equation [10], nonlinear Schrödinger equation [11], and integrable evolution equations [40].

Finally, all these examples can be subdivided into two classes: in the first, the domain size is prescribed and so plays the role of an external parameter; in the second, the domain size is determined as part of the solution. Although many of these problems, like that due to Stefan [109], have been formulated a long time ago, most are far from being solved and require the development of new mathematical techniques in order to obtain better insight into the physical mechanisms responsible for the often fascinating behavior they exhibit.

2 Key Physical Examples

In what follows, we discuss representative physical examples from various fields illustrating different types of phenomena whose dynamics, including bifurcations and stability properties, depend strongly on the time variation of the spatial domain. As often happens, it is the simplest possible example which provides us with the most physical insight and helps us to develop intuition. The level of detail provided below assumes basic erudition on the reader's part in both physics and mathematics, while further details can be found in the cited literature. The following examples are organized by their dynamics type: examples from fluid dynamics, astrophysics, control, fluid-structure interaction, wave equations, and quantum mechanics deal with *oscillatory* or *wave* behavior, while examples on reaction-diffusion and solidification systems are of *diffusion* type.

2.1 Fluid Dynamics

Fluid flows with a free or moving solid-fluid interface provide natural examples of systems on time-dependent spatial domains, as exemplified by the drop splash problem leading to the famous problem of crown formation—a pattern formed on an evolving rim (Fig. 1). Despite recent progress in understanding the bifurcation picture behind this phenomenon from both experimental [46, 59] and theoretical [55, 58] perspective, this problem remains unsolved

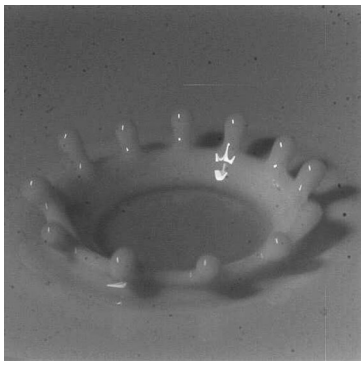

Fig. 1 Crown formation in the drop splash problem [59]

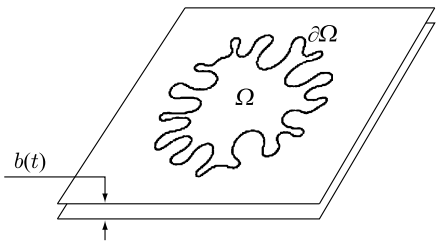

Fig. 2 A schematic diagram of a drop in a Hele-Shaw cell

from a quantitative point of view. We therefore describe a number of simpler, representative systems illustrating the behavior resulting from the time-dependence of the spatial domain. For relevant function-analytic studies of the existence and regularity of solutions of the equations of fluid dynamics we refer the reader to [48, 117] for the Euler equation and [12, 35, 79, 111] for the Navier-Stokes equation.

Hele-Shaw Cell with a Time-Dependent Gap [105] We consider a drop of viscous fluid between two parallel plates one of which is being raised. This causes the drop to retract resulting in a variant of the Saffman-Taylor instability [102], which can be described by a version of Darcy's law in two dimensions, where the divergence (mass conservation) condition is modified to account for the lifting of the plate, cf. Fig. 2. The use of Darcy's law implies that the plate is neither being lifted fast enough to provoke any inertial effects nor being lifted high enough to violate the assumption of a thin layer. The system of governing equations reads

$$\mathbf{u} = -\frac{b^2(t)}{12\nu}\nabla p \quad \text{in } \Omega(t), \tag{1a}$$

$$\nabla \cdot \mathbf{u} = -\frac{\dot{b}(t)}{b(t)} \quad \text{in } \Omega(t), \tag{1b}$$

$$p = \tau\kappa \quad \text{on } \partial\Omega(t), \tag{1c}$$

$$v_n = -\frac{b^2(t)}{12\nu}\frac{\partial p}{\partial n} \quad \text{on } \partial\Omega(t). \tag{1d}$$

Equation (1a), where $\mathbf{u}$ is the two-dimensional gap-averaged velocity, p the pressure, $b(t)$ the (prescribed) time-dependent gap width, and ν the fluid viscosity, represents Darcy's law.

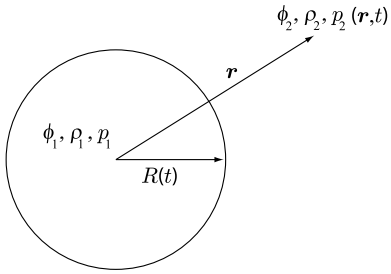

Fig. 3 A schematic of a spherical bubble in an infinite liquid

Equation (1b) expresses conservation of volume for the fluid mass, and is a modification of the usual two-dimensional divergence-free condition. We take the traditional Laplace-Young boundary condition for the pressure (1c), where τ is the surface tension and κ is the curvature of $\partial\Omega(t)$. Finally, in Eq. (1d) v_n is the normal component of the boundary velocity and $\mathbf{n}$ is the outward unit normal vector to $\partial\Omega(t)$. Condition (1d) thus requires that the boundary $\partial\Omega(t)$ moves with the fluid.

To explore the effects of time-dependence in this system, consider the flow resulting from perturbation of an exact solution in the form of an expanding or contracting 2D circular drop of radius, $R(t) = R(0)\sqrt{b(0)/b(t)}$. Infinitesimal radial perturbations of this state with integer azimuthal wavenumber $k \geq 2$, $\alpha(t,\theta) = \widehat{\alpha}(t)\exp ik\theta$, obey a nonautonomous linear equation that can be obtained from the system (1a)–(1d):

$$\frac{\mathrm{d}\widehat{\alpha}}{\mathrm{d}t} = \sigma(t,k)\widehat{\alpha}, \tag{2}$$

where $\sigma(t,k)$ is the instantaneous growth rate given by [105]

$$\sigma(t,k) = \frac{k}{2}\frac{\dot{b}}{b} + \frac{b^2}{R^3}\widetilde{\tau}\left(k-k^3\right), \quad k \geq 2, \tag{3}$$

and $\widetilde{\tau}$ is a suitably chosen nondimensionalized surface tension. One is tempted [105] to conclude that the circular drop is stable provided $\sigma(t,k) < 0$, suggesting that a circular drop is linearly stable at all scales if $\dot{b} < 0$, i.e., if the drop is expanding; note that since the wavenumber k is necessarily an integer, only wavenumbers $k \geq 2$ are relevant, because infinitesimal perturbations with wavenumbers $k = 0$ and $k = 1$ correspond to deformations that maintain the circular shape of the drop (which is displaced from the origin in the case of $k = 1$). For these perturbations the surface tension drops out, and the growth rate (3) is either zero or negative whenever $\dot{b} < 0$. In contrast, if the drop is contracting, Eq. (3) suggests that it is linearly unstable for $k < \sqrt{1 + (\dot{b}R^3)/(2\widetilde{\tau}b^3)}$. However, time-dependent problems of this type require care [55]. First, depending on the function $b(t)$, one may have instability even when the time-frozen "eigenvalue" oscillates between positive and negative values, since the time integral of $\sigma(t,k)$ may nonetheless be positive (see the Appendix). If, however, one is interested in the long-time behavior, i.e., stability of the zero solution to (2), then one can apply standard theorems from theory of ordinary differential equations (ODEs) [51] to conclude that the general solution to (2) cannot remain bounded for all times $t \geq a$ if the integral $\int_a^\infty \sigma(t,k)\mathrm{d}t$ diverges. Second, the onset of the instability is delayed—a key effect also discussed in the Appendix.

Spherical Bubble Dynamics [98] Let us consider the dynamics of a 3D bubble (Fig. 3) when the inner and outer phases are both inviscid and in potential motion, i.e., there exists

a velocity potential ϕ such that $\mathbf{u} = \nabla\phi$. Choosing a velocity potential corresponding to a disturbance which decays away from the interface in both the inward and outward directions, one obtains

$$\phi_1 = \left(R^2\dot{R}\right)/r + b_1 r^n Y_n, \quad r < R, \tag{4a}$$

$$\phi_2 = \left(R^2\dot{R}\right)/r + b_2 Y_n/r^{n+1}, \quad r > R, \tag{4b}$$

where Y_n is the spherical harmonic of degree n and the quantities $b_{1,2}$ are determined from the continuity of the velocity at the distorted interface $r_s = R + aY_n$ with $|a(t)| \ll R(t)$. In the case where the surface tension can be neglected both inner and outer pressures are equal as determined from Bernoulli's equation, and the evolution of the amplitude $a(t) \equiv (R_0/R)^{3/2}\alpha$ can be found from a second order differential equation for α,

$$\ddot{\alpha} = \sigma(t)\alpha, \tag{5}$$

where for $\rho_1 \gg \rho_2$:

$$\sigma(t) = \frac{3}{4}\frac{\dot{R}^2}{R^2} - \frac{\ddot{R}}{R}\left[n + \frac{1}{2}\right]. \tag{6}$$

For second order nonautonomous ODEs of type (5) a standard theorem [8, 51] states that the two independent solutions of (5) cannot be both bounded as $t \to \infty$ if $\sigma(t) > 0$ for all $t > 0$. In the present case one concludes that the bubble (drop) is necessarily unstable if $\ddot{R} < 0$, a result similar to the Rayleigh-Taylor instability [29], although instability is possible even if $\ddot{R} > 0$ provided it remains small enough so that $\sigma(t) > 0$ for all $t > 0$. The resulting growing surface corrugations are ultimately responsible for the bubble disintegration. If, however, $\sigma(t) < 0$ for all t, then the solutions of (5) are of oscillatory type, cf. [51].

Shallow-Water Waves [18, 45] Water waves represent rich phenomena on time-varying spatial domains. As an example, let us consider the (inviscid) shallow-water (long-wave) system over variable depth $h(x, y)$:

$$\frac{\partial u}{\partial t} + u\frac{\partial u}{\partial x} + v\frac{\partial u}{\partial y} + g\frac{\partial \eta}{\partial x} = 0, \tag{7a}$$

$$\frac{\partial v}{\partial t} + u\frac{\partial v}{\partial x} + v\frac{\partial v}{\partial y} + g\frac{\partial \eta}{\partial y} = 0, \tag{7b}$$

$$\frac{\partial \eta}{\partial t} + \frac{\partial}{\partial x}\big[(\eta + h)u\big] + \frac{\partial}{\partial y}\big[(\eta + h)v\big] = 0, \tag{7c}$$

where u and v are the velocity components in a Cartesian (x, y)-frame of reference and $\eta(t, x, y)$ represents surface elevation (Fig. 4). The first two equations describe linear momentum conservation in the x and y directions, respectively, while the last equation is a consequence of mass conservation. Linearizing (7a)–(7c) about a fluid at rest, $(\eta, u, v) = (0, 0, 0)$, we arrive at a 2D wave equation for the surface displacement:

$$\frac{\partial^2 \eta'}{\partial t^2} = \nabla \cdot \left[c^2 \nabla \eta'\right], \tag{8}$$

where $c = c(x, y) \equiv \sqrt{gh}$ depends explicitly on the varying bottom topography $h = h(x, y)$. This is a good model for the propagation of a tsunami across the open ocean, with typical

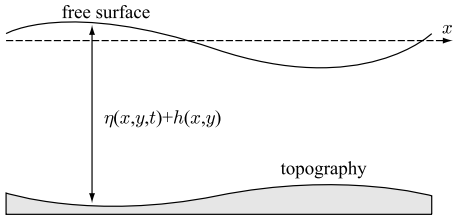

Fig. 4 A schematic illustration of the shallow-water system: both the surface elevation η and the depth h are measured from the undisturbed surface; the y-coordinate is orthogonal to the page plane

depth h_0 of order 4 km and tsunami wavelength ~ 100 km, leading to the following estimate of the group speed, $c_g \sim \sqrt{gh_0} = 200$ m/s. The variation of the depth in the direction of wave propagation can be seen as an example of a system with time-varying domain—the depth changes as the wave propagates towards the shore. Close to the shore, the wave compresses horizontally and its height increases. This process can be described within linear theory if the near-shore topography varies sufficiently slowly; in other cases the linear approximation breaks down and a nonlinear description becomes necessary. Of course, in situations involving rapid temporal changes in topography, such as those occurring during earthquakes or landslides, one may also consider a time-dependent depth $h(t, x, y)$.

2.2 Astrophysics

The Friedmann Model [42] This classical model describes the scaling of key (cold matter and radiation) densities ρ in the Universe with its expansion factor, which is time-dependent. To illustrate the main features of the model, let us write down the equations that govern the evolution of the mean properties of the Universe. First of all, the co-moving separation, $\overline{x}$, which factors out the expansion of the Universe, is related to physical separation $\overline{r}$ through $\overline{r} = a(t)\overline{x}$, where $a(t)$ is the scale (expansion) factor of the Universe (equal to unity today) and related to the redshift z by $a = 1/(1+z)$. On large scales, the Universe is expanding with the relative velocity of two co-moving objects proportional to their physical separation by $\overline{u} = H(t)\overline{r}$, with the factor H being the Hubble parameter. From the above relations it is easy to show that $H = \dot{a}/a$. The Friedmann equations are derived from Einstein's equations and account for the evolution of H and $\overline{\rho}$:

$$\left(\frac{\dot{a}}{a}\right)^2 + \frac{kc^2}{a^2} = \frac{8\pi}{3}G\overline{\rho} + \frac{\Lambda c^2}{3}, \tag{9a}$$

$$\frac{\ddot{a}}{a} = \dot{H} + H^2 = -\frac{4\pi G}{3}\left(\overline{\rho} + \frac{3\overline{p}}{c^2}\right) + \frac{\Lambda c^2}{3}, \tag{9b}$$

where k is the curvature, $\overline{\rho}$ the mass-energy density, $\overline{p}$ the pressure, Λ the cosmological constant, and c the speed of light in vacuum. The first law of thermodynamics, $\mathrm{d}U + \overline{p}\mathrm{d}V = 0$, implies that

$$\frac{\mathrm{d}\overline{\rho}}{\mathrm{d}t} + 3H\left(\overline{\rho} + \frac{\overline{p}}{c^2}\right) = 0, \tag{10}$$

which can be easily integrated to show that the density for nonrelativistic (cold) matter, $\overline{\rho}_m \propto a^{-3}$, whereas for relativistic particles or radiation, $\overline{\rho}_r \propto a^{-4}$.

In addition to the above effect of the Universe expansion (domain time-dependence) on the densities, one can also use this model to show that these time-dependent but spatially uniform densities may experience instabilities responsible for the large-scale structure of

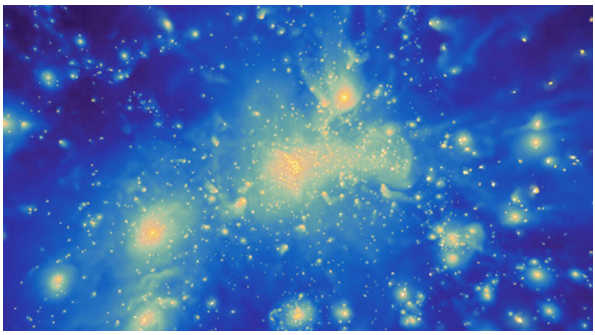

Fig. 5 Large-scale structure of the Universe: evolution of the gas density in the Bolshoi cosmological simulation of the evolution of the large-scale structure of the Universe [47]

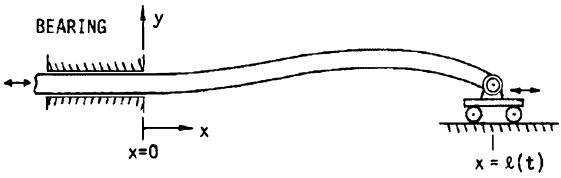

Fig. 6 Extensible flexible beam with a simply supported movable end

the Universe [94], as shown in Fig. 5, via the appearance of the Jeans instability [50], which causes the collapse of interstellar gas clouds and subsequent star formation. This instability occurs when the internal gas pressure is not strong enough to prevent gravitational collapse of a region filled with matter. More generally, hydrodynamics in an expanding Universe obeys nonautonomous Navier-Stokes equations depending on $a(t)$, a fact that has a profound influence on hydrodynamic stability and the properties of turbulence [54].

2.3 Control

Distributed systems with time-dependent spatial domains arise naturally in many physical situations. Often, it is desirable to control [5, 89, 121] the dynamical behavior of such systems by varying their spatial domain. To illustrate the basic ideas, we give a simple concrete example.

Vibration Control of an Extensible Flexible Beam [121] Figure 6 shows an extensible flexible beam whose right end is supported on a movable base, while its left end is embedded inside a bearing which permits extension and contraction of the beam. Neglecting the effect of axial acceleration on the vibrations of the beam, the inplane bending motion of the beam $y = y(t, x)$ is described by

$$\rho y_{tt} + (EIy_{xx})_{xx} = 0, \quad 0 < x < l(t), \tag{11}$$

where $\rho = \rho(x)$ denotes the mass of the beam per unit length, $EI = EI(x)$ is the flexural rigidity, and $l(t)$ is the length of the beam at time t. The boundary conditions at the left end are given by

$$y(t, 0) = 0, \qquad y_x(t, 0) = 0, \tag{12}$$

while those at the right end are

$$y\big(t, l(t)\big) = 0, \qquad (EIy_{xx})_x\big(t, l(t)\big) = 0. \tag{13}$$

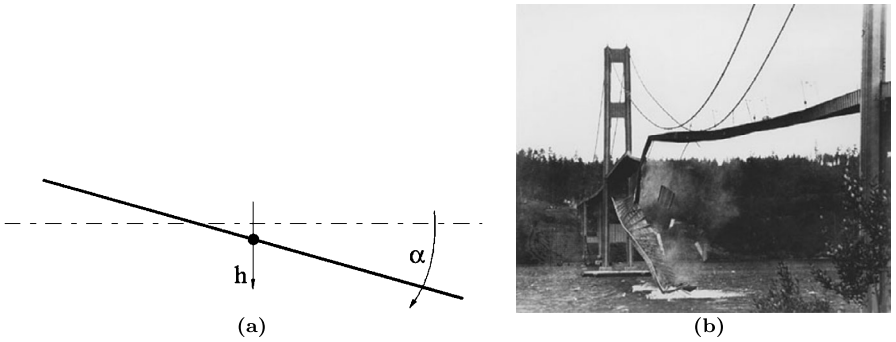

Fig. 7 Flutter: (**a**) degrees of freedom for flutter analysis, (**b**) the collapse of the Tacoma Narrows Bridge in 1940

The initial conditions at $t = 0$ are specified by

$$y(0, x) = y_0(x), \qquad y_t(0, x) = y_1(x), \quad x \in \big[0, l(0)\big]. \tag{14}$$

Assuming that extension or contraction of the beam is achieved by a linear actuator, the beam's length $l = l(t)$ obeys

$$M\ddot{l}(t) + \nu\dot{l}(t) = f_c(t), \tag{15}$$

where M is the total effective mass of the beam and the actuator and ν is the friction coefficient. From the applied point of view, it is of interest to find an appropriate control law f_c to move the beam from an initial length $l(0)$ to a given desired length l_d without inducing excessive beam vibrations. The foregoing simple example illustrates a situation where the spatial domain of a distributed system is time-dependent. Moreover, the control affects the domain motion, which is governed by an ordinary differential equation (15). This class of systems also includes large space structures with deployable elastic components [81].

2.4 Fluid-Structure Interaction

Fluid-structure interaction (FSI) problems [37] are common in nature, and include the biomechanics of birds, fish, heart valves, arteries, etc. Understanding and accurate prediction of FSI responses is also important to many engineered structures, such as bridges, tall buildings, rotor blades, spars, sails, and membranes, in order to avoid potential aeroelastic/hydroelastic instability issues [52, 100], or to improve performance by actively and/or passively tailoring the structural morphology. Much of the early work on FSI problems focused on aerospace structures, where the effects of fluid damping and fluid inertia could be approximated or ignored. We consider here the classical example of FSI—flutter.

Flutter The flutter phenomenon is the most-widely treated problem in aeroelasticity. This is perhaps due to the violent nature of the instability, which makes predicting its occurrence a necessity in aircraft as well as in bridge design. Analytical flutter analysis for design purposes today is still performed by means of relatively simple analytical methods the most important of which can be illustrated with the following equations of motion for the translational and torsional degrees of freedom, respectively, cf. Fig. 7(a):

$$m\ddot{h} + 2m\zeta_h\omega_h\dot{h} + m\omega_h^2 h = F_h(t), \tag{16a}$$

$$I\ddot{\alpha} + 2m\zeta_\alpha\omega_\alpha\dot{\alpha} + I\omega_\alpha^2 h = F_\alpha(t). \tag{16b}$$

Here the driving forces F_h and F_α for heave and pitch are governed by the aerodynamics of the body and thus by the displacements of the section. A popular approach to flutter analysis is due to Theodorsen [112], who investigated flutter of aircraft wings. Everyday exhibition of flutter includes flag flapping [4].

As an interesting historical note, one should mention that the first hypothesis for the failure of the Tacoma Narrows bridge (Fig. 7(b)) was resonance, because it was thought that the Kármán vortex street frequency was the same as the torsional natural vibration frequency. This proved to be incorrect as the actual failure was due to aeroelastic flutter [9].

2.5 Wave Equation and Oscillations

While a concrete example will be discussed in detail later, in Sect. 4.1, here we would like to mention a few key works and results on the vast subject of wave equations on time-dependent domains [41], which is of both practical and theoretical interest. From a practical view point, a vibrating string being lengthened or shortened in the manner in which a violinist produces vibrato, Fermi accelerators [36], and electromagnetic cavity resonators serve as motivating examples. Of main theoretical interest is the construction of analytic solutions, where key contributions are due to Balazs [6], who also introduced graphical methods of solution. These methods were subsequently extended by many authors, e.g. [43, 63, 101, 106]. The main concern is the possible instability of solutions, i.e., unbounded energy growth. For example, the work of Gonzalez [44] showed that energy remains bounded for the wave equation with Dirichlet boundary conditions in a time-varying domain $0 < x < a(t)$ with $a(t)$ assumed to move slower than the wave speed. But, in general, instability may take place as happens, for example, for the classical, periodically driven string [27]. As was shown by Cooper [16], the energy growth of the solution caused by a periodically moving boundary occurs because of the compression of the wave, and not by amplification as one would naturally expect. The instability of the solutions of the wave equation can also be studied with the help of spectral methods as illustrated with a simple example below.

The Spectrum of a Hyperbolic Evolution Operator [17] Consider the boundary value problem for $u(t, x)$ on $\Sigma = \{(t, x) : 0 < x < s(t)\} \in \mathbb{R}^2$:

$$u_{tt} - u_{xx} = 0 \quad \text{in } \Sigma, \tag{17a}$$

$$u = 0 \quad \text{on } \partial\Sigma. \tag{17b}$$

If we consider the time T-map U which maps initial data $\{u(0), u_t(0)\}$ to the solution and its derivative $\{u(T), u_t(T)\}$ of the homogeneous wave equation in a domain with a T-periodic boundary, e.g. $s(t) = 1 + \epsilon \sin \pi t$ with period $T = 2$ and $\epsilon\pi < 1$ (so that $|\dot{s}| < 1$, a condition required for the well-posedness of (17a)–(17b)), then the spectrum of U is the annulus

$$\left\{\lambda \in \mathbb{C} : \frac{1}{\sqrt{a}} \le |\lambda| \le \sqrt{a}\right\}, \tag{18}$$

where the two circles $|\lambda| = \sqrt{a}$ and $|\lambda| = 1/\sqrt{a}$ represent continuous spectrum. If λ lies in the open annulus between the circles, then $U - \lambda I$ has a closed range with infinite co-dimension. Moreover, if the solution u is not identically zero, then

$$\lim_{\pm\infty} |t|^{-1} \ln\left(\|u(t)\|_{H^1} + \|u_t(t)\|_{L^2}\right) = \ln a/4, \tag{19}$$

i.e., the "energy" (in these Sobolev norms) grows without bound. This example also illustrates the fact that even though by a change of variables one can view this problem as a nonautonomous problem on a fixed domain, the spectrum consisting of an annulus and nonexistence of eigenvalues precludes application of standard Floquet theory. As shown by Lopes [70], this occurs because the characteristics may converge as $t \to \infty$.

A closely related problem, that of a vibrating extensible beam, was considered by Dickey [26], Ball [7], Ferreira et al. [38] and others.

2.6 Quantum Mechanics

The behavior of particles in time-dependent potential wells is a subject that is closely related to the properties of the wave equation on a time-dependent domain discussed above. Quantum systems with an explicit time-dependent Hamiltonian have attracted much attention over the past decades. In addition to their intrinsic mathematical importance, these systems connect to several important physical problems such as quantum optics, Paul electromagnetic traps for charged and neutral particles [93], Berry phase, and magnetic field lens. Of considerable interest is the escape of particles from a time-dependent potential well [23]—in their seminal work Büttiker and Landauer [15] considered tunneling through a time-modulated barrier, and found that at high frequencies the particle passes through the time-averaged potential inelastically, losing or gaining modulation quanta. In general, this problem belongs to a class of questions about energy transfer in classical systems [64], i.e., whether a particle, that can give up or absorb energy from the system, can be accelerated to unlimited energy [36].

Schrödinger Equation on Time-Dependent Domains The time-dependent Schrödinger equation

$$i\hbar\frac{\partial\psi}{\partial t} = H\psi \quad \text{with } H = -\frac{\hbar^2}{2m}\frac{\partial^2}{\partial x^2} + V(x), \tag{20}$$

where the potential

$$V(x) = \begin{cases} 0, & x \in [0, L(t)] \\ \infty, & x \notin [0, L(t)] \end{cases} \tag{21}$$

describes the problem of a particle in a one-dimensional infinite square-well potential with a moving wall. Following the idea of instantaneous energy eigenfunctions by Schiff [103], Doescher and Rice [28] found an exact solution to this problem in the case when $\mathrm{d}L/\mathrm{d}t =$ const:

$$\psi(t, x) = \sum_n a_n \phi_n(t, x), \tag{22}$$

where the $\phi_n(t, x)$ are time-dependent eigenfunctions given by

$$\phi_n(t, x) = (2/L)^{1/2} \exp\left[i\alpha\xi\left(\frac{x}{L}\right)^2 - in^2\pi^2\frac{(1 - 1/\xi)}{4\alpha}\right] \sin\frac{n\pi x}{L(t)}, \tag{23}$$

with $\alpha = L_0(m/2\hbar)\mathrm{d}L/\mathrm{d}t$, $\xi = L(t)/L_0$, $L_0 = L(0)$, and the expansion coefficients a_n remain constant as the wall moves. Note that the eigenfunctions $\phi_n(t, x)$ stay normalized as

the wall moves and form a complete orthogonal set. As in the case of time-independent eigenfunctions, the constants a_n are determined by the value of the wave function at $t = 0$:

$$a_n = \int_0^{L_0} \psi_n^*(0, x)\psi(0, x)\mathrm{d}x. \tag{24}$$

The motivation for studying such systems comes from the question of transitions between energy states when the system is "shaken". After the work of Doescher and Rice [28], many other authors extended their results. In particular, Makowski and Dembiński [77, 78] found a solution for (21) using separation of variables valid for $L^3\ddot{L} = \text{const}$ as well as for the case where the bottom of the infinite square potential well is not at zero, but oscillates up and down as in the Fermi-Ulam accelerator model [36] (i.e. a particle bouncing between two impenetrable rigid walls one of which moves as a function of time):

$$V(t, x) = \frac{1}{2}m\Omega^2(t)x, \qquad \Omega^2(t) = \frac{Q\sin\omega t}{L(t)}\omega^2. \tag{25}$$

This system exhibits chaotic behavior when $L(t)$ is a periodic function of time [67], since in contrast to autonomous one-degree-of-freedom systems nonautonomous one-degree-of-freedom systems (sometimes called one and a half degrees of freedom systems because the relevant phase space is three-dimensional) permit chaos as external forcing destroys the conserved quantity given by the Hamiltonian.

To see the basic effect the moving wall has on the system, let us transform Eq. (20) following the change of variables in [77, 83]:

$$y = \frac{x}{L(t)}, \qquad \psi(t, y) = \sqrt{\frac{2}{L}}\exp\left(\frac{im}{2\hbar}L\dot{L}y^2\right)\phi(t, y), \qquad \tau(t) = \int_0^t \frac{\mathrm{d}s}{L^2(s)}, \tag{26}$$

which gives

$$i\hbar\frac{\partial\phi}{\partial\tau} = -\frac{\hbar^2}{2m}\frac{\partial^2\phi}{\partial x^2} + \left(\frac{1}{2}mL^3\ddot{L}y^2 + L^2V\right)\phi, \tag{27}$$

i.e. the transformation introduces a time-dependent perturbation to the potential and thus to the Hamiltonian [60], which makes the subject related to general studies of systems with nonautonomous Hamiltonians, e.g. [15, 53, 108]. Existence of exact solutions was later related to a certain invariance of the Schrödinger equation under scaling of the space and time coordinates or, equivalently, the existence of time-dependent invariants [82]. For the details of the classical perturbative treatment of the Schrödinger equation with time-dependent perturbations, $H = H_0 + V(t)$, the reader is referred to Landau and Lifshitz [60]. The basic idea, however, is straightforward and supposes that the solution of the perturbed Schrödinger equation can be constructed in the form $\psi = \sum_k a_k(t)\psi_k^{(0)}$, where $\psi_k^{(0)}$ are the wavefunctions of the unperturbed Schrödinger equation. Substituting this representation in the Schrödinger equation (20) and taking into account that $\psi_k^{(0)}$ satisfy

$$i\hbar\frac{\partial\psi_k^{(0)}}{\partial t} = H_0\psi_k^{(0)}, \tag{28}$$

we find

$$i\hbar\sum_k \psi_k^{(0)}\frac{\mathrm{d}a_k}{\mathrm{d}t} = \sum_k a_k V\psi_k^{(0)}. \tag{29}$$

Next, projecting on $\overline{\psi}_k^{(0)}$ and integrating, we obtain a system of equations for $a_k(t)$:

$$i\hbar\frac{\mathrm{d}a_m}{\mathrm{d}t} = \sum_k V_{mk}(t)a_k, \qquad V_{mk}(t) = \int \overline{\psi}_k^{(0)} V \psi_k^{(0)} \mathrm{d}x, \tag{30}$$

the solution of which allows one to determine wavefunctions for the perturbed motion. One must note that in general one cannot speak of perturbations of the energy eigenvalues because the energy is not conserved for time-dependent Hamiltonians. Below, we will elaborate on several concrete examples of perturbed Hamiltonian systems in both classical and quantum settings.

Development of perturbation methods for problems with moving walls has been pursued in [25, 28, 96] and compared with exact treatment, revealing serious limitations of the approximate methods [96]. However, interesting results were obtained, for example, in the case of asymptotic (long-time) behavior [25]. Besides systems with potential wells, whose width changes in time, there is also work on moving potential wells, e.g. on conveyance of quantum particles in such systems [80] and noise-activated escape from a sloshing potential well [76]. Ratcheting, resulting in net motion, was found in a periodic array of potential wells with spatially symmetric barriers pulsating periodically in time [99]. And, finally, there are studies on the escape of noninteracting particles from the inside of an infinite potential box which, in turn, contains a time-dependent potential well (i.e., a well within a well), e.g. [23, 65].

Classical and Quantum Time-Dependent Harmonic Oscillators Let us consider a system with a Hamiltonian of the form

$$H = \frac{1}{2\epsilon}\left[p^2 + \Omega^2(t)q^2\right], \tag{31}$$

where q is a canonical coordinate, p is the conjugate momentum, $\Omega(t)$ is an arbitrary function of t, and ϵ is a positive real parameter. As originally established by Lewis [66], for this time-dependent harmonic oscillator there is a class of exact invariants I of the form

$$I = \frac{1}{2}\left[\rho^{-2}q^2 + \left(\rho p - \epsilon\rho' q\right)^2\right], \tag{32}$$

where ρ is any function of t satisfying

$$\epsilon^2\rho'' + \Omega^2(t)\rho - \rho^{-3} = 0, \tag{33}$$

and the prime denotes differentiation with respect to t. The quantity I is a time-dependent invariant for quantum as well as classical systems. As shown by Lewis [66] the invariant may be used to solve the time-dependent Schrödinger equation.

Transitions Induced by Time-Dependent Potentials As a simple model for vibrational excitation induced by a compression pulse applied to a harmonic oscillator which increases its force constant, let us consider the following time-dependent Hamiltonian

$$H(t) = \frac{p^2}{2m} + \frac{1}{2}k(t)x^2. \tag{34}$$

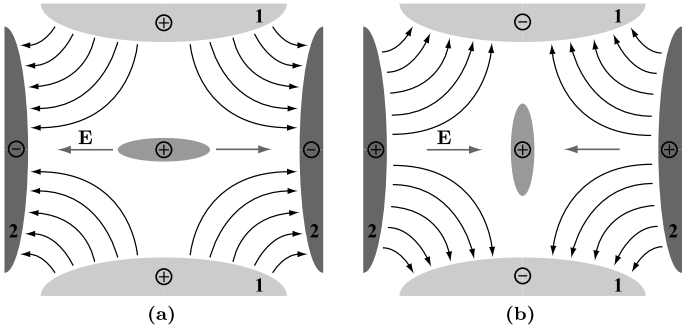

Fig. 8 Schema of a quadrupole ion trap with a particle of positive charge (*center*), surrounded by a cloud of similarly charged particles. The electric field **E** is produced by a quadrupole generated by the endcaps **1** and a ring electrode **2**. Panels **a** and **b** show two states during an AC cycle

The compression pulse can be seen as a change in the potential well width, i.e., the domain size in our terms. Taking out the harmonic oscillator part H_0 of $H(t) = H_0 + V(t)$ by partitioning the time-dependent force constant into two parts $k(t) = k_0 + \delta k(t)$ with $k_0 = m\Omega^2$ and $\delta k(t) = \delta k_0 \exp\left(-\frac{(t-t_0)^2}{2\sigma^2}\right)$, we can find the eigenstates of H_0, $H_0|n\rangle = E_n|n\rangle$:

$$H_0 = \hbar\Omega\left(a^\dagger a + \frac{1}{2}\right), \qquad E_n = \hbar\Omega\left(n + \frac{1}{2}\right). \tag{35}$$

Using first-order perturbation theory [60] and calculating the wavefunction expansion amplitudes

$$b_n(t) = -\frac{i}{2\hbar}\int_{t_0}^{t} V_{n0}(\tau)e^{i\omega_{n0}\tau}\mathrm{d}\tau, \qquad \omega_{n0} = (E_n - E_0)/\hbar = n\Omega, \qquad V_{0n} = \langle 0|V(t)|n\rangle,$$

we can determine the probability of finding the system in state $|n\rangle$ after applying the perturbation to it in state $|0\rangle$: $P_n = |b_n|^2$. For example, for $n = 2$ we find

$$P_2 = \frac{\pi\delta k_0^2\sigma^2}{2m^2\Omega^2}e^{-4\sigma^2\Omega^2}, \tag{36}$$

which indicates that significant transfer from the state $|0\rangle$ to $|n\rangle$ occurs when the compression pulse width is small compared with the vibration period, $\sigma \ll \Omega^{-1}$, i.e., the potential is changing faster than the atoms can respond to the perturbation. In the opposite (adiabatic) limit, $\sigma \gg \Omega^{-1}$, the perturbation is so slow that the system always remains in the state $|0\rangle$.

Chirped Frequency Excitation A chirped frequency ω_p is an excitation frequency that varies with time, typically linearly. Recent years have seen increasing use of chirped frequencies in a number of applications, ranging from plasma physics [33] and quantum state measurement [85] to the recent successful trapping of antihydrogen atoms [2], cf. Fig. 8. When a nonlinear physical system such as a particle trapped in a potential or a nonlinear pendulum is perturbed by a force with a chirped frequency, the natural frequency of the system can lock to ω_p. In this case the driving frequency "drags" the natural frequency with it, i.e., the amplitude of the oscillation of the system adjusts itself in such a way that resonance is maintained. This locking occurs abruptly above a critical amplitude of the perturbation

in a phenomenon known as autoresonance [32, 86]. In a *soft* system, i.e., a system whose natural frequency decreases with oscillation amplitude, a downward sweep of the driving frequency ω_p decreases the oscillation frequency and hence increases its amplitude. Conversely, in a *hard* system an upward sweep of the driving frequency is required to increase its amplitude. This behavior persists in the presence of damping [34]. The success of this technique suggests that similar behavior may be present in problems described by PDEs instead of ODEs, i.e., in pattern-forming systems. To illustrate the effect of a chirped frequency compared with that of a standard resonance, consider the following driven linear oscillator model

$$\ddot{x} + \gamma \dot{x} + \omega_0^2 x = \sin(\omega_f t), \tag{37}$$

where γ is a damping coefficient, ω_0 is the natural frequency without damping, and ω_f is a forcing frequency. The standard resonance occurs when the forcing frequency ω_f is constant and equal to $\omega_n = \sqrt{\omega_0^2 - \gamma^2/4}$ and leads to oscillations with maximum amplitude

$$A \sim \frac{1}{\omega_n}\left(1 + \frac{\gamma^2}{8}\right). \tag{38}$$

If, however, the forcing frequency varies slowly in time, $\omega_f(t) = \omega_{f0} + \epsilon t$ with $|\epsilon| \ll 1$, then as shown in [92] the resonance occurs at the *jump* frequency

$$\omega_j \simeq \frac{\omega_{f0} + \omega_n}{2} \quad \text{and is reached at} \quad t_j = \frac{1 - \omega_{f0}}{2\epsilon}, \tag{39}$$

i.e., at the midfrequency between the initial frequency ω_{f0} and the natural frequency ω_n, and the maximum amplitude at this chirped resonance scales as $A \sim \epsilon^{-1/2}$ with the ramp speed ϵ. This highlights the difference from the static driving frequency problem: resonance phenomena occur prior to the slowly varying frequency reaching its critical value in the corresponding static-frequency problem.

2.7 Reaction-Diffusion Systems

There is a large number of biological processes involving time-dependent domains, namely the formation of patterns and shapes in biology (morphogenesis) [19, 84, 88, 119]. The latter phenomena include mammalian coat patterns, seashell pigmentation patterns and skin patterns on tropical fish, as well as various symmetry-breaking events: branching processes in plants, initiation of single or multiple new organs in animals, and solid tumor growth. As suggested by Turing [114], pattern formation in biology can be modeled by a system of reacting and diffusing chemicals (morphogens) that interact to produce stable patterns of morphogen concentrations $\mathbf{c}(\boldsymbol{x}, t)$ as described by the reaction-diffusion model $\mathbf{c}_t = \mathbf{D} \cdot \Delta \mathbf{c} + \boldsymbol{f}(\mathbf{c})$, where $\mathbf{D}$ is a matrix of diffusion coefficients and $\boldsymbol{f}$ is a reaction term. Such models are known to be able to capture complex evolving patterns arising from a competition between reactions that create spikes in the concentration of the product and diffusion that smooths out its gradient. Recent interest has focused on incorporating other biologically relevant features such as domain growth, shape, and curvature into models of this type [19, 88].

Morphogenesis [19, 20, 73, 74, 91, 114, 115] Let us consider the nonautonomous reaction-diffusion system [19]

$$\frac{\partial c}{\partial t} = \frac{1}{\gamma} D \frac{\partial^2 c}{\partial x^2} + R(c), \quad x \in [0, 1] \tag{40}$$

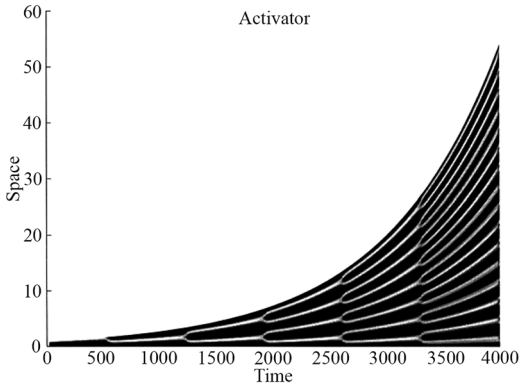

Fig. 9 The wavenumber-doubling sequence: space–time evolution of the activator concentration profile [19]

with zero flux boundary conditions and initial condition $c(0,x)$, and suppose that the dimensionless scaling parameter γ evolves according to $\mathrm{d}\gamma/\mathrm{d}t = h(t)$ with $\gamma(0) = \gamma_0$. Then for a suitable $h(t)$ the concentration $c(t,x)$ can exhibit self-similar wavenumber-doubling in space (Fig. 9). To see this we assume that $\gamma(t)$ is a monotonically increasing function so that we can eliminate t in favor of γ; then at $\gamma = \gamma^*$ the solution has some spatial profile $c(\gamma^*, x)$. At any point in the wavenumber-doubling sequence, in particular at $\gamma = \gamma^*$, a pattern of twice the wavenumber may be constructed by applying the tent map

$$p_2(x) = \begin{cases} 2x, & 0 \le x \le \frac{1}{2}, \\ 2 - 2x, & \frac{1}{2} \le x \le 1. \end{cases} \tag{41}$$

We define $q_2(\gamma, x)$ such that $q_2(\gamma', x) \equiv c(\gamma', p_2(x))$, which satisfies the evolution equation

$$h(\gamma')\frac{\partial q_2}{\partial \gamma'} = \frac{1}{4\gamma'} D \frac{\partial^2 q_2}{\partial x^2} + R(q_2). \tag{42}$$

Returning to the original equation, $c(4\gamma', x)$ is governed by

$$\frac{1}{4} h(4\gamma')\frac{\partial c}{\partial \gamma'} = \frac{1}{4\gamma'} D \frac{\partial^2 c}{\partial x^2} + R(c). \tag{43}$$

Now $c(4\gamma', x)$ and $q_2(\gamma', x)$ satisfy the same equation if

$$h(4\gamma') = 4h(\gamma'), \tag{44}$$

i.e., $\gamma(t) \propto e^{2\alpha t}$ or equivalently $L(t) = L_0 e^{\alpha t}$, for some $\alpha > 0$, where $L(t)$ is the domain size. In this (special) case every cell splits simultaneously and in an identical fashion, cf. Fig. 9.

2.8 Solidification

Mullins-Sekerka Instability [61] As another example of a parabolic system, let us consider the key interfacial instability driving pattern formation during solidification, cf. Fig. 10. The following simple analysis applies to both thermal and chemical models, so we consider a dimensionless diffusing field u. Denoting the diffusion constants in the liquid and solid by D and D', respectively, the continuity condition reads

$$v_n = D\big[\beta(\nabla u)_{\text{solid}} - (\nabla u)_{\text{liquid}}\big] \cdot \mathbf{n}, \tag{45}$$

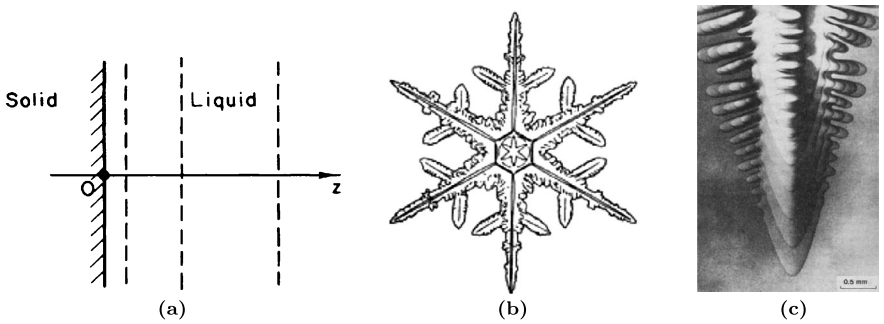

Fig. 10 Examples of the Mullins-Sekerka instability [61]: (**a**) schematic, (**b**) snow flake, (**c**) succinonitrile

where the left-hand side is the rate v_n (the velocity directed in the normal direction $\mathbf{n}$ to the interface) at which, say, heat is generated at the interface and the right-hand side is the rate at which this heat flows into the bulk phases on either side of the interface. Introducing the capillary length d_0 and the interfacial curvature κ, the Gibbs-Thomson condition [24] can be written as

$$u_{\text{interface}} = -d_0\kappa, \tag{46}$$

which accounts for the variations in chemical potential across a curved interface and, in particular, a reduction of the melting temperature for small particles—this is opposed to assuming that the temperature at the interface must be exactly the bulk melting temperature as in the Stefan problem to be discussed below. In the frame of reference moving in the z direction at the interface velocity v, the steady-state diffusion equation has the form

$$\nabla^2 u + \frac{2}{l}\frac{\partial u}{\partial z} = 0, \tag{47}$$

where l is the diffusion length, $l = 2D/v$ (in the solid, $l = 2D'/v$). The interface is placed at $z = 0$. The solution of (47) and the continuity condition (45) is

$$u_0 = \exp\left(-\frac{2z}{l}\right) - 1 \quad (\text{liquid},\ z \geq 0), \tag{48a}$$

$$u_0' = 0 \quad (\text{solid},\ z \leq 0). \tag{48b}$$

Next, we introduce a perturbation of the steady-state interface $\zeta(\mathbf{x}, t) = \widehat{\zeta}_{\mathbf{k}} \exp(i\mathbf{k}\cdot\mathbf{x} + \omega_k t)$, where $\mathbf{k}$ is a two-dimensional wavevector perpendicular to $\mathbf{n}$ and ω_k is the amplification rate, and the corresponding perturbations u' to the field u_0:

$$u = \exp\left(-\frac{2z}{l}\right) - 1 + \widehat{u}_{\mathbf{k}} \exp(i\mathbf{k}\cdot\mathbf{x} - qz + \omega_k t) \quad (\text{liquid},\ z \geq 0), \tag{49a}$$

$$u' = \widehat{u}'_{\mathbf{k}} \exp\left(i\mathbf{k}\cdot\mathbf{x} + q'z + \omega_k t\right) \quad (\text{solid},\ z \leq 0). \tag{49b}$$

Linearizing (45)–(47), we determine the dispersion relation

$$\omega_k \simeq kv\left[1 - \frac{1}{2}(1+\beta)d_0 l k^2\right], \tag{50}$$

consisting of two parts: a positive, destabilizing term, which is proportional to the velocity, and a negative, stabilizing term, which contains surface tension. The wavenumber k_s at which ω_k vanishes, i.e., the neutral stability point, sets a pattern-formation length scale for the problem $\lambda_s \equiv 2\pi/k_s \simeq 2\pi\sqrt{ld_0(1+\beta)/2}$.

It is interesting to mention that a famous application of the Mullins-Sekerka theory is to the familiar surface instability of icicles, though not so long time ago it was realized that the underlying physical mechanisms are different [90].

Stefan Problem [109] The original Stefan problem treats the formation of ice in the polar seas [109]. In fact, Stefan compared his mathematical results with measurements performed during polar expeditions to find the North-West passage [120].

Let us consider the second model described by Stefan [109], in which the unsteady transport of heat in ice is taken into account. In the ice layer the temperature difference between the freezing temperature and that of the ice satisfies the following partial differential equation

$$\frac{\partial u}{\partial t} = \frac{K}{c\sigma}\frac{\partial^2 u}{\partial x^2}, \quad 0 < x < h(t),\ t > 0, \tag{51}$$

where $h(t)$ is the layer depth and $h(0) = 0$. At the air-ice interface the temperature is a given function of t, i.e., $u(t,0) = f(t)$, whereas at the ice-water interface the temperature is equal to the temperature of freezing, i.e., $u(t,h(t)) = 0$. The boundary condition at the ice-water interface $x = h(t)$ follows from heat balance:

$$\lambda\sigma\frac{\mathrm{d}h}{\mathrm{d}t} = -K\frac{\partial u}{\partial x}, \quad t > 0. \tag{52}$$

When $f(t) = \alpha$ the solution to (51), (52) is

$$h(t) = 2\mu\sqrt{\frac{Kt}{c\sigma}}, \qquad u(t,x) = \alpha\int_{x/2\sqrt{\frac{Kt}{c\sigma}}}^{\mu} e^{-z^2}\mathrm{d}z \Big/ \int_0^{\mu} e^{-z^2}\mathrm{d}z, \tag{53}$$

where μ is the solution of the transcendental equation $\mu e^{\mu^2}\int_0^{\mu} e^{-z^2}\mathrm{d}z = \alpha c/(2\lambda)$.

The Stefan problem stimulated many interesting studies. Beginning with Petrovskii's paper [95], a significant attention has been on boundary value problems for parabolic equations in non-cylindrical domains (i.e., time-dependent spatial domains as usually referred to in the context of parabolic systems) with a singular point, at which the boundary surface is tangent to the hyperplane perpendicular to the t-axis (notice that the initial condition for the domain size in the Stefan problem is $h(0) = 0$). For example, in problems described by the heat equation in domains in $\mathbb{R}^n$ with an insulated rapidly moving boundary, heat will tend to collect at the boundary and the temperature will rise, while the medium will cause that energy to diffuse away from the boundary and thus lower the temperature. One of the interesting facts is that if the boundary moves fast enough, namely if $h(t) \sim (T-t)^{-1/2}$ for $t \sim T$, singularities can develop in the solution such that the boundary point will contain a positive amount of heat in the distribution (generalized function) sense, and form a so-called "heat atom". The resulting heating can be analyzed using the theory of reflecting Brownian motion, cf. [13, 14, 68, 107], known in probability theory as the Skorokhod problem for stochastic differential equations with a reflecting boundary condition [107].

3 Mathematical Formulation

3.1 General Setting: Evolution of Conserved Quantities on Time-Dependent Domains

It is natural to start with a general evolution equation on a time-independent domain:

$$\frac{\partial c}{\partial t} = \mathcal{L}_{\mathbf{x}} c + N(c), \qquad N(0) = 0, \tag{54}$$

where c is a quantity originating from some conservation law, e.g. concentration, $\mathcal{L}_{\mathbf{x}}$ is a constant coefficient time-independent differential operator in the spatial variable $\mathbf{x}$ (in the case of a reaction-diffusion system $\mathcal{L}_{\mathbf{x}} = D\nabla^2$), and $N(c)$ is a general nonlinear differential operator, which may originate from the nonlinear part of the reaction term. However, in many cases equations of this type are usually the result of the application of a conservation law [19, 110]. In the case of a general time-dependent domain Ω_t, the time derivative is

$$\frac{\mathrm{d}}{\mathrm{d}t}\int_{\Omega_t} c(t,\mathbf{x})\mathrm{d}\mathbf{x} = \int_{\Omega_t}\left[\frac{\partial c(t,\mathbf{x})}{\partial t} + \nabla\cdot(\mathbf{u}c)\right]\mathrm{d}\mathbf{x}, \tag{55}$$

after application of the Reynolds transport theorem, implying that the correct form of the evolution equation is

$$\frac{\partial c}{\partial t} + \nabla\cdot(\mathbf{u}c) = \mathcal{L}_{\mathbf{x}} c + N(c), \qquad N(0) = 0, \tag{56}$$

where $\mathbf{u}(t,\mathbf{x})$ is the velocity of the domain point at $(t,\mathbf{x})$. Thus the evolution of the quantity c is considered on a time-deforming domain Ω_t, which could be thought of as a 'substrate': examples include reaction-diffusion on growing skin, crown-spike structure on a growing circular rim in the drop splash problem, waves in a stretching rod, etc. The growth of the domain Ω_t introduces an advection term, $\mathbf{u}\cdot\nabla c$, corresponding to elementary volumes moving with the flow $\mathbf{u}(t,\mathbf{x})$, and a dilution term, $c\nabla\cdot\mathbf{u}$, due to local volume change. Note that $\mathbf{u}(t,\mathbf{x})$ is characterized by a magnitude as well as a lengthscale and timescale on which it operates—these are to be determined in the process of deduction. Note that the Reynolds theorem (55) applies only to problems defined on domains of the same dimension as the space in which they are embedded; if one considers evolution of a quantity on a line embedded in 2D or 3D or evolution on a 2D surface embedded in 3D, there is an additional term related to the deformation of that surface [97, 104] as will be illustrated in Example 3 of Sect. 3.2.

In 1D, the time rate of change of the quantity $c(t,x)$ can be analyzed with the help of the Leibnitz rule:

$$\begin{aligned}\frac{\mathrm{d}}{\mathrm{d}t}\int_{\alpha(t)}^{\beta(t)} c(t,x)\mathrm{d}x &= \int_{\alpha(t)}^{\beta(t)}\frac{\partial c}{\partial t}\mathrm{d}x + c(t,\beta)\dot{\beta}(t) - c(t,\alpha)\dot{\alpha}(t)\\ &= \int_{\alpha(t)}^{\beta(t)}\frac{\partial c}{\partial t}\mathrm{d}x + c(t,\beta)u|_{x=\beta} - c(t,\alpha)u|_{x=\alpha} = \int_{\alpha(t)}^{\beta(t)}\left(\frac{\partial c}{\partial t} + \frac{\partial(uc)}{\partial t}\right)\mathrm{d}x,\end{aligned}$$

leading to the same result as (56).

3.2 On the Flow $\mathbf{u}(t,\mathbf{x})$ from the Lagrangian and Eulerian Viewpoints

Let us adopt Lagrangian (material) coordinates (t,a) for the time-dependent motion of a cross-section labeled by a at $t = 0$ and displaced by $H(t,a)$ for $t > 0$, cf. Fig. 11. The

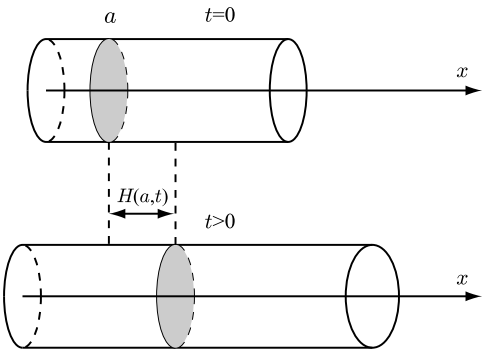

Fig. 11 Domain stretching illustrated using a rod with (t, a) as the Lagrangian variables and (t, x) as the Eulerian variables; $H(t, a)$ is the displacement of a cross-section labeled by the Lagrangian variable a for $t > 0$

Eulerian variables (t, x) are given by

$$x = X(t, a), \qquad X(0, a) = a, \tag{57}$$

via the displacement $H(t, a) = X(t, a) - a$, so that $H(0, a) = 0$. The velocity of the cross-section labeled by a in the Lagrangian variables is

$$U(t, a) = \frac{\partial X}{\partial t}. \tag{58}$$

The corresponding Eulerian variables are determined after inversion of $x = X(t, a)$, i.e., first finding $a = a(t, x)$, so that the velocity and the displacement are given by

$$u(t, x) = U\big(t, a(t, x)\big), \qquad h(t, x) = H\big(t, a(t, x)\big). \tag{59}$$

It is important to keep in mind that the label a is defined on a fixed interval, e.g. $0 \le a \le l_0$, while x is, in general, defined on the stretched time-dependent interval, $X(t, 0) \le x \le X(t, l_0)$.

Consider a general function $F(t, a)$ in Lagrangian coordinates with its Eulerian counterpart $f(t, x) = f(t, X(t, a)) = F(t, a(t, x))$. Differentiating both sides with respect to time t, we find

$$\frac{\mathrm{d}f}{\mathrm{d}t} = \frac{\partial f}{\partial t} + \frac{\partial f}{\partial x}\frac{\partial X}{\partial t} = \frac{\partial f}{\partial t} + U(t, a)\frac{\partial f}{\partial x} = \frac{\partial f}{\partial t} + u(t, x)\frac{\partial f}{\partial x}, \tag{60}$$

where we took into account that $U(t, a) = u(t, x)$. As a consequence, for $f(t, x) = h(t, x)$ the Eulerian velocity $u(t, x)$ is the material derivative of $h(t, x)$, i.e., $u(t, x) = \mathrm{d}h/\mathrm{d}t$, and not $\partial h/\partial t$; thus $u(t, x) = h_t/(1 - h_x)$. A nice example [49] to test all the above properties is $x = a(1 + 2t)/(1 + t)$, which allows one to calculate the relevant quantities explicitly, i.e., $a(t, x)$, $h(t, x)$, etc. The above discussion readily generalizes to the vector case.

Example 1 (Isotropic Growth) In one spatial dimension, $X(t, a) = a\xi(t)$ with $\xi(t)$ a dimensionless scale factor satisfying $\xi(0) = 1$ and $a \in [-L_0/2, L_0/2]$, implying that

$$u(t, x) = a\dot{\xi} = x\frac{\dot{\xi}}{\xi}, \tag{61}$$

i.e., there is a stationary point $x = 0$ away from which the domain is stretching with $L(t) = L_0\xi(t)$ being the total domain length and maximum stretch velocity at the domain

boundaries $x = \pm L(t)/2$ being $u = \pm L_0\dot{\xi}/2 = \pm\dot{L}/2$. A physical example would be an elastic stretched by pulling both ends with the same velocity, but in opposite directions. In general, of course, this kind of stretching is not necessarily linear in x, but depends on the elastic properties of the domain. In any event, for the flow (61) we have the material derivative

$$\frac{\partial c}{\partial t} + \frac{\partial}{\partial x}(uc) = \frac{\partial c}{\partial t} + \frac{\dot{\xi}}{\xi}x\frac{\partial c}{\partial x} + \frac{\dot{\xi}}{\xi}c \tag{62}$$

i.e., both advection and dilution are present, though the advection term can be removed by transforming back to the Lagrangian coordinate, $x \to a = x/\xi(t)$, as in [19, 116]. One may ask when does this type of advective flow become a function of time only, i.e., $u = u(x)$? Equation (61) shows that this is the case when the domain grows exponentially, $\xi \sim e^{\alpha t}$. Hence, while the class of isotropically growing domains corresponds to $u(t, x) = f(t)x$ with $f(t) = \dot{\xi}/\xi = \dot{L}/L$, exponentially (and isotropically) growing domains belong to an important subclass, characterized by $f(t) = \text{const}$. Pattern formation on exponentially growing domains was studied numerically in several articles [19, 72, 74, 115].

Example 2 (Translation-Invariant Systems) In the above example the point $x = 0$ is special since the advection velocity vanishes there. Thus problems with isotropic stretch break translation invariance (as does the presence of the boundaries at $x = \pm L(t)/2$). Translation-invariant systems are different since all their spatial locations are equivalent. In such systems the (Eulerian) advection velocity u must be independent of the (Eulerian) spatial coordinate, and so $u \equiv 0$ everywhere. In this case only *homogeneous* stretching remains, and any two points in the domain move apart with a Lagrangian velocity proportional to their separation similar to the expansion of the Universe in the Friedmann model, cf. Sect. 2.2. In this context it is helpful to think in terms of points on the surface of an expanding ring or balloon. For example, in the crown formation problem [55, 59], shown in Fig. 1, the system is posed on a one-dimensional domain with periodic boundary conditions. Because of translation invariance (modulo the period) there is no preferred location and so $u \equiv 0$ everywhere.

Example 3 (Reaction-Diffusion Equation on a Uniformly Growing Ring) The discussion given thus far relates the presence of dilution to an Eulerian advection velocity u. As indicated in the preceding example this velocity vanishes in a translation invariant system, suggesting that in such systems dilution is absent as well. This is not necessarily the case, however.

Consider the scalar reaction-diffusion equation on an expanding ring of radius $R(t)$ as in the crown formation problem. We may use polar coordinates and a *two-dimensional* advection velocity $\mathbf{u} = (u(r, t), 0)$ to obtain the Eulerian equation for the evolution of the concentration $c = c(t, \theta)$ per unit length concentrated at $r = R(t)$:

$$\frac{\partial c}{\partial t} + \nabla \cdot (\mathbf{u}c) = \nabla^2 c + s(c), \tag{63}$$

or, equivalently,

$$\frac{\partial c}{\partial t} + \frac{c}{r}\frac{\partial}{\partial r}(ru) = \frac{1}{r^2}\frac{\partial^2 c}{\partial \theta^2} + s(c). \tag{64}$$

For perimeter length $L(t) = 2\pi R(t)$, we have $u = \dot{R}$ and hence

$$\frac{\partial c}{\partial t} + \frac{\dot{R}}{r}c = \frac{1}{r^2}\frac{\partial^2 c}{\partial \theta^2} + s(c). \tag{65}$$

The reaction-diffusion equation *along* the ring of radius $r = R$ is therefore

$$\frac{\partial c}{\partial t} + \frac{\dot{R}}{R}c = \frac{1}{R^2}\frac{\partial^2 c}{\partial \theta^2} + s(c). \tag{66}$$

Since the physical coordinate is $x = R\theta$, the required Eulerian equation satisfied by c is

$$\frac{\partial c}{\partial t} + \frac{\dot{L}}{L}c = \frac{\partial^2 c}{\partial x^2} + s(c), \quad -\frac{L}{2} \le x < \frac{L}{2}, \tag{67}$$

and dilution is present even though Eulerian advection along the ring is absent.

Therefore, in the crown problem, illustrated in Fig. 1, we also expect to see a dilution effect, although it competes with the (mass) source term s. In the simplest case one may suppose that the mass is supplied from the fluid bulk at a rate that balances the dilution effect, allowing the crown to develop on top of this balanced state [55]. In any case, experiments suggest that the crown instability occurs on a faster time scale than that on which the dilution and source terms affect the base state [59].

It is worthwhile to compare Eq. (67) with that obtained in the case of isotropic Eulerian stretch velocity $u = \dot{L}(t)x/L(t)$ on a domain $[-L/2, L/2]$ with (say) Neumann boundary conditions. From (56), (61) we have

$$\frac{\partial c}{\partial t} + \frac{\dot{L}}{L}x\frac{\partial c}{\partial x} + \frac{\dot{L}}{L}c = \frac{\partial^2 c}{\partial x^2} + s(c), \quad -\frac{L}{2} \le x < \frac{L}{2}, \tag{68}$$

an equation that superficially resembles (67), in the sense that the dilution terms $(\dot{L}/L)c$ are the same. However, this statement is misleading since the origin of the dilution term is now the isotropic Eulerian stretch and not the fact that c is a density with conserved total mass.

3.3 Nonconserved Systems

Not all physical systems lead to conserved dynamics. Consider, for example, gravity-capillary waves on the surface of a slowly draining tank of water. The frequency ω and (horizontal) wavenumber k of the (inviscid) waves are related by the dispersion relation $\omega^2 = gk \tanh hk$, where h is the liquid depth and g is the acceleration due to gravity. As h varies with time, the oscillation frequency will drift (since the wavenumber is fixed by the Neumann boundary conditions imposed on the lateral walls—this spatial quantization comes from the fact that problems with the Neumann boundary conditions can be embedded into ones with periodic boundary conditions on domains of twice the size modulo translation). Conversely, if the waves are excited by parametric forcing, their frequency will be fixed, but the wavenumber will vary (abruptly) with time. In a finite domain this time-dependence will generate a sequence of jumps in the wavenumber very similar to the phase slips discussed in Sect. 4.2. Since the (horizontal) domain is unstretched, advection and dilution effects are absent from the equations describing this class of problems.

In the more realistic viscous setting the above picture will change because the required non-Neumann boundary conditions no longer fix a wavenumber [21], thereby allowing a continuous evolution of the solution in time.

4 Dynamics

To deepen our understanding of the key new effects observed in problems on time-dependent domains compared with those on time-independent domains, we now discuss in detail two

representative physical examples: propagation of waves in extensible bodies and the evolution of spatially periodic patterns. This will also help set the stage for open questions in this evolving area of research.

4.1 Longitudinal Waves in a Stretching Rod

Consider propagation of longitudinal waves in a rod which is being stretched, cf. Fig. 11. In what follows we reveal two key effects: (1) if the rod ends are pulled in opposite directions with the same velocity $\alpha(t)$ proportional to time, then the wavelength of the longitudinal waves propagating in the rod due to an initial 'kick' (not deflection, but velocity) grows in proportion to α, and (2) if $\ddot{\alpha} \neq 0$, then long waves are excited in the rod even without an initial 'kick', i.e., when the rod is not subject to an initial displacement and velocity perturbation.

4.1.1 Analysis in Lagrangian Variables

Suppose that the rod cross-sections (Lagrangian coordinates) are labeled by $a \in [0, l_0]$ and that the left and right ends of the rod are pulled with the same velocity, but in opposite directions, so that the corresponding displacements $H(t, a)$ are

$$a = 0: \; H(t, 0) = -\alpha(t), \tag{69a}$$

$$a = l_0: \; H(t, l_0) = \alpha(t), \tag{69b}$$

where $\alpha(0) = 0$. In Lagrangian variables the linear elasticity (momentum) equation reads

$$R_0 \frac{\partial^2 H}{\partial t^2} = E \frac{\partial^2 H}{\partial a^2}, \tag{70a}$$

$$t = 0: \; H(0, a) = 0, \quad H_t(0, a) = \psi(a), \tag{70b}$$

where E is Young's modulus, $\psi(0) = \psi(l_0) = 0$ (the compatibility of initial and boundary conditions is necessary for the existence of a classical solution) and $R_0 = R(0, a)$ is the initial density distribution in Lagrangian variables; density at later times is determined by $R(t, a) = R_0(a)/(1 + H_a)$ with $H_a = \partial H/\partial a$. Representing $H(t, a)$ in the form $H(t, a) = \widetilde{H}(t, a) + \kappa(a)\alpha(t)$ with $\kappa(a) = -1 + (2/l_0)a$, we arrive at the following boundary-initial value problem:

$$R_0 \frac{\partial^2 \widetilde{H}}{\partial t^2} = E \frac{\partial^2 \widetilde{H}}{\partial a^2} - R_0 \kappa(a) \ddot{\alpha}, \tag{71a}$$

$$t = 0: \; \widetilde{H}(0, 0) = 0, \quad \widetilde{H}_t(0, a) = \widetilde{\psi}(a), \tag{71b}$$

$$a = 0: \; \widetilde{H}(0, t) = 0, \tag{71c}$$

$$a = l_0: \; \widetilde{H}(l_0, t) = 0. \tag{71d}$$

In the case $\alpha \propto t$ the resulting solution is

$$\widetilde{H}(t, a) = \sum_{n=1}^{\infty} \frac{\widetilde{\psi}_n}{\omega_n} \sin \omega_n t \sin \sqrt{\lambda_n} a, \tag{72}$$

where $\omega_n = \frac{\pi cn}{l_0}$, $\lambda_n = \left(\frac{\pi n}{l_0}\right)^2$, $c = \sqrt{E/R_0}$ and $\widetilde{\psi}_n = \frac{2}{l_0}\int_0^{l_0} \widetilde{\psi}(\xi)\sin\sqrt{\lambda_n}\xi \mathrm{d}\xi$. To understand this solution in Eulerian variables, notice that $x = X(t,a) = H(t,a) + a = \widetilde{H}(t,a) + \kappa(a)\alpha(t) + a$, which needs to be inverted to get $a(t,x)$ so that the displacement reads $h(t,x) = H(t,a(t,x))$. In general, this inversion is not possible analytically, but for small $\widetilde{H}$ one obtains $h(t,x) = H(t,a(t,x))$, with a defined by

$$x = \left(-1 + \frac{2}{l_0}a\right)\alpha(t) + a \Rightarrow a = \frac{x + \alpha(t)}{1 + \frac{2}{l_0}\alpha(t)}. \tag{73}$$

For $\alpha(t) \gg l_0$ we obtain $a \simeq \frac{l_0}{2}[\frac{x}{\alpha(t)} + 1]$. Hence the wave frequencies ω_n are unaffected by the stretching (ω_n is independent of $\alpha(t)$), but the wavelength of the waves grows in proportion to $\alpha(t)$.

If α is not a linear function of time, the problem (71a)–(71d) admits a nontrivial solution even without a 'kick', i.e., when $\widetilde{\psi} = 0$. These waves are driven by the acceleration of the boundaries and given by

$$\widetilde{H}(t,a) = \int_0^t \int_0^{l_0} G(t-\tau, a, b) f(\tau, b)\mathrm{d}b\mathrm{d}\tau, \tag{74}$$

where $f(t,a) = -\kappa(a)\ddot{\alpha}(t)$ and the Green's function

$$G(t-\tau,a,b) = \sum_{n=1}^{\infty} \frac{2}{\pi nc}\sin\frac{\pi na}{l_0}\sin\frac{\pi nb}{l_0}\sin\omega_n(t-\tau), \quad c = \sqrt{E/R_0}. \tag{75}$$

4.1.2 Analysis in Eulerian Variables

The conclusion reached above that the wavelength of the waves grows in proportion to $\alpha(t)$ can also be reached from an Eulerian analysis, although it is more complicated as the resulting elasticity equations, namely the continuity and momentum equations

$$\frac{\partial \rho}{\partial t} + \frac{\partial}{\partial x}(u\rho) = 0, \tag{76a}$$

$$\rho\left(\frac{\partial u}{\partial t} + u\frac{\partial u}{\partial x}\right) = \frac{\partial \tau}{\partial x}, \tag{76b}$$

respectively, are nonlinear, which illustrates the difference between the Lagrangian and Eulerian approaches. Here $u = h_t/(1-h_x)$ and the stress $\tau = Eh_x/(1-h_x)$. Only in the linear approximation, i.e., when $h(t,x)$ is small, one can use the linear wave equation resulting from (76a)–(76b),

$$\rho_0 h_{tt} = Eh_{xx}, \tag{77a}$$

$$x = -\alpha(t):\ h = -\alpha(t), \tag{77b}$$

$$x = l_0 + \alpha(t):\ h = \alpha(t), \tag{77c}$$

$$t = 0:\ h = 0, \quad h_t = \phi(x). \tag{77d}$$

Assuming that $\alpha(t)$ evolves on a slower time scale and making the transformation $(t,x) \to (\tau = t, \xi = (x+\alpha)/(1+2\alpha/l_0))$, $h = \widetilde{h} + (-1 + 2\xi/l_0)\alpha(t)$, we arrive at

$$\rho_0 \widetilde{h}_{\tau\tau} = \frac{E}{\left(1 + \frac{2\alpha}{l_0}\right)^2}\widetilde{h}_{\xi\xi}, \tag{78a}$$

$$\xi = 0 : \ \widetilde{h} = 0, \tag{78b}$$

$$\xi = l_0 : \ \widetilde{h} = 0, \tag{78c}$$

the solution of which for $\alpha \gg l_0$ also demonstrates wavelength stretching at the rate $\alpha(t)$ since $\xi \simeq \frac{l_0}{2}(1 + x/\alpha)$.

4.2 Pattern Formation: Eckhaus Instability

A central question concerning pattern formation in systems on time-dependent domains is how the domain deformation affects periodic structures. This question is somewhat analogous to the question of how the quasistatic variation of a bifurcation parameter affects the properties of a periodic structure on time-independent domains [30]. The key insight is provided by the Eckhaus instability whereby the system can respond to a stretching (contracting) domain by inserting (annihilating) a wavelength. To understand how this occurs we consider the Ginzburg-Landau equation (GLE) for a complex order parameter A on both time-independent and time-varying domains.

4.2.1 Time-Independent Domain

We begin with a review of the Eckhaus instability on a finite fixed length domain [30] and consider the supercritical Ginzburg-Landau equation,

$$\partial_t A = \mu A + \partial_x^2 A - |A|^2 A, \tag{79}$$

which governs the formation of steady patterns in a wide variety of systems [22]. Here $t \equiv \epsilon^2 \widetilde{t}$ and $x \equiv \epsilon \widetilde{x}$ with $|\epsilon| \ll 1$ are slow temporal and spatial scales, i.e., the complex amplitude $A(t, x)$ describes the slow spatial modulation of the basic periodic state $u(\widetilde{t}, \widetilde{x})$,

$$u(\widetilde{t}, \widetilde{x}) = \epsilon A\big(\epsilon^2 \widetilde{t}, \epsilon \widetilde{x}\big) e^{i q_c \widetilde{x}} + \epsilon \overline{A}\big(\epsilon^2 \widetilde{t}, \epsilon \widetilde{x}\big) e^{-i q_c \widetilde{x}} + \text{h.o.t.}, \tag{80}$$

where q_c is the (critical) wavenumber at the pattern-forming instability, the tildes indicate the original (fast) variables, and $\overline{A}$ stands for the complex conjugate of A. If the domain is infinite, q_c is an arbitrary real number; if, however, the domain is of finite length L (in the slow coordinate x), then q_c is given in units of $2\pi\epsilon/L$ and is an integer for spatially periodic systems.

In general, if the state with wavenumber q_c is stable so are the states with nearby wavenumbers. These are described by a periodic amplitude function,

$$A_Q(x) = a_Q e^{iQx}. \tag{81}$$

Solutions of this type exist provided $|a_Q|^2 = \mu - Q^2 > 0$; the latter inequality defines the region of existence of these so-called phase-winding solutions in the (μ, Q) plane. The solutions are shown in Fig. 12(a) and correspond to periodic patterns with (unscaled) spatial wavenumber $q_c \pm \epsilon Q$; they appear via a supercritical pitchfork bifurcation at $\mu_Q = Q^2$ meaning that as μ increases past $\mu = 0$ the trivial state is destabilized and patterns with Q in the range $(0, \sqrt{\mu})$ are created. If the domain is finite, the wavenumber Q is also an integer in units of $2\pi/L$.

Linear stability of the pattern A_Q is studied by writing $A(t, x) = A_Q(x) + A'(t, x)$, leading to the linearized version of Eq. (79),

$$\partial_t A' = \mu A' + \partial_x^2 A' - \big[2|A_Q|^2 A' + A_Q^2 \overline{A}'\big]. \tag{82}$$

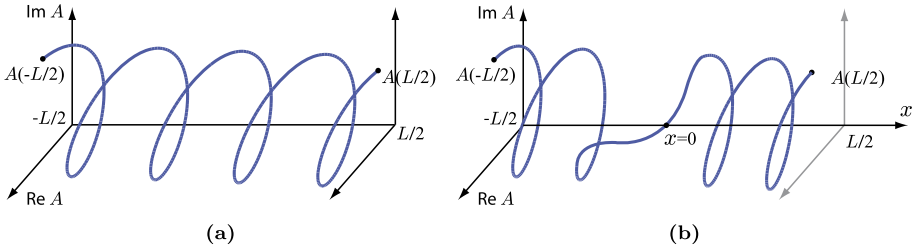

Fig. 12 A phase slip event: (**a**) the periodic order parameter A, (**b**) phase slip event at $t = t^*$, $x = 0$

With the perturbation represented as

$$A'(t,x) = e^{iQx}\left[a_{k+}(t)e^{ikx} + \overline{a}_{k-}(t)e^{-ikx}\right] \quad \text{for } k \neq 0, \tag{83}$$

this gives us two equations for the amplitudes $a_{k\pm}$ of the harmonics $e^{i(Q\pm k)x}$:

$$\frac{\mathrm{d}a_{k+}}{\mathrm{d}t} = \left(\mu - (Q+k)^2\right)a_{k+} - a_Q^2(2a_{k+} + a_{k-}), \tag{84a}$$

$$\frac{\mathrm{d}a_{k-}}{\mathrm{d}t} = \left(\mu - (Q-k)^2\right)a_{k-} - a_Q^2(2a_{k-} + a_{k+}), \tag{84b}$$

where we used the fact that a_Q may be taken to be real, so that $|a_Q|^2 = a_Q^2$. The associated eigenvalues are given by $\lambda_{k\pm} = -(\mu - Q^2) - k^2 \pm \sqrt{(2Qk)^2 + (\mu - Q^2)^2}$, where λ_{k-} is always negative and λ_+ crosses zero when

$$\mu = \mu_{Qk} \equiv 3Q^2 - \frac{1}{2}k^2, \qquad k \neq 0. \tag{85}$$

At $\mu = \mu_{Qk}$ a secondary pitchfork bifurcation occurs from the branch of states A_Q, cf. Fig. 13(b). In the case $k = 0$, the solution is sought in the form $A'(t,x) = a_0(t)e^{iQx}$, which yields the eigenvalue $\lambda_0 = -2(\mu - Q^2)$; since $\lambda_0 < 0$ for $\mu > Q^2$, this eigenvalue is responsible for the creation of A_Q from the trivial state. The pattern described by A_Q is stable when all the eigenvalues, λ_0 and $\lambda_{k\pm}$, are negative, which yields the classical Eckhaus curve (E) shown in Fig. 13(a) in the case of an infinite domain:

$$\mu_\infty = \max_{k>0}\left(3Q^2 - \frac{1}{2}k^2\right) = 3Q^2, \tag{86}$$

as can also be seen from the leading eigenvalue expanded for small k:

$$\lambda_{k+} = \frac{3Q^2 - \mu}{\mu - Q^2}k^2 + \text{h.o.t.} \tag{87}$$

It follows that as μ increases past successive values μ_{Q_k}, the solution A_Q is stabilized against A' as λ_{k+} decreases through zero. Thus in the case of an infinite domain, $L = \infty$:

- the fastest growing wavenumber $k_{\max} \to 0$ as $Q \to \sqrt{\mu_\infty/3}$;
- the spatially periodic (base) state (81) exists for $Q^2 < \mu$;
- the base state (81) of (79) is stable in the region $3Q^2 < \mu$ and unstable in the region $Q^2 < \mu < 3Q^2$;

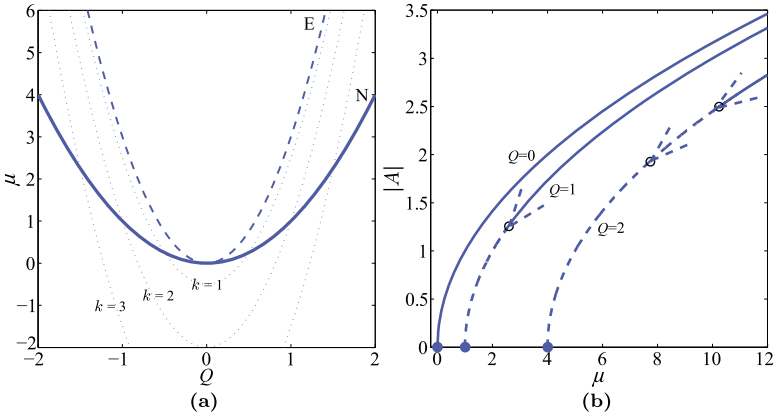

Fig. 13 On the Eckhaus stability [113]. (**a**) The trivial state $A = 0$ loses stability along the *solid curve* (N), $\mu_Q = Q^2$; *the dashed curve* (E) defined by $\mu_\infty = 3Q^2$ represents the stability boundary on an infinite domain; the dotted curves represent loci of the Eckhaus instability on a finite periodic domain—the case $k = 1$ corresponds to the finite-domain Eckhaus boundary above which the pattern A_Q is stable. (**b**) Branches with wavenumbers $Q_j = j$ are created at successive pitchfork bifurcations (*solid dots*) as μ increases through the values Q_j^2. All but the first branch are initially unstable, but each $j = 1, \ldots$ branch acquires stability at a secondary Eckhaus bifurcation (*open circles*) at $\mu_{Qk} = 3Q^2 - \frac{1}{2}k^2$. *Solid* (*dashed*) *curves* indicate stable (unstable) portions of the trivial and primary branches

– in addition, the Eckhaus bifurcation is subcritical [113], meaning that the spatially modulated wavetrain created by the instability lies *inside* the curve E and is therefore *unstable*.

These conclusions are represented graphically in Fig. 13(a). To interpret the Eckhaus instability one may also think in terms of a single wavenumber Q:

– at a given positive μ, there is a range of possible Q's, $Q^2 < \mu$;
– suppose we fix a solution A_Q with a particular Q in this range and increase μ—initially the solution lies between the (N) and (E) curves and so is unstable;
– once μ reaches $3Q^2$, the solution A_Q acquires stability w.r.t. all perturbations with wavenumbers $Q \pm k$, cf. (87).

In the unstable region bounded by the curves E and N in Fig. 13(a), the perturbations a_{k+}, a_{k-} grow exponentially and quickly become nonlinear. This growth drives the amplitude A locally to zero, cf. Fig. 12(b); at such locations the phase of the solution is undefined, as can be seen from the explicitly constructed solution at the phase-slip, cf. Eq. (89) below, allowing the phase to jump by $\pm 2\pi$ [31, 57, 62].

Thus phase slips are associated with the appearance of zeros in the solution of a nonlinear parabolic PDE (79), a process studied in [3, 31]. As established by Eckmann et al. [31], if one starts from the generic (in appropriate topology) initial condition 'just before' the phase slip,

$$A(0, x) = \frac{1}{2}ax^2 + ibx - ad \equiv A_0(x), \tag{88}$$

where $a > 0$ and $d(a, b) > 0$ is sufficiently small, i.e., the initial condition has a nonzero slope b and small curvature a as can be observed in Fig. 12(b), then at leading order a phase slip occurs at time $t^* = d$ and location $x^* = 0$. This result is proved using well-known

regularity properties of parabolic equations and thus looking for a solution in the form

$$A(t,x) = A_0(x) + ct, \tag{89}$$

where c proves to be equal to a. In addition to this *local theory*, one can also prove a *global* result, namely that when one starts the system in an unstable state a phase slip inevitably results [31].

On the other hand, in the case of a finite domain, $L < \infty$, one has

$$\mu_{\text{finite}} = \max_{k=1,2,\ldots} \left(3Q^2 - \frac{1}{2}k^2\right) = 3Q^2 - \frac{1}{2} = \mu_\infty - \frac{1}{2}, \tag{90}$$

a result independent of the actual size of the domain [57, 113] as experimentally observed by Ahlers et al. [1]. Here, keeping in mind (80), we took into account that the periodic pattern A_Q permitted on finite domains must satisfy $\epsilon^{-1}q_c + Q \in \mathbb{Z}$ in units of $2\pi/L$; potentially unstable eigenvectors a_k must also fit in the domain, so that k must satisfy $\epsilon^{-1}q_c + Q + k \in \mathbb{Z}$, i.e., k must be a (positive) integer too. Besides the finiteness of the domain, the boundary conditions have a significant effect on both the existence of periodic patterns and the perturbations since they limit the class of possible solutions as shown for a semi-infinite domain in [56].

For the details on how phase-slips occur dynamically, we refer the reader to [57, 62]. On a time-independent periodic domain the GLE (79) may be stated in the variational form

$$\frac{\partial A}{\partial \tau} = -\frac{\delta \mathcal{F}}{\delta A^*}, \qquad \mathcal{F} = \int_{-L_0/2}^{L_0/2} \left(\left| \frac{\partial A}{\partial \xi} \right|^2 - \mu |A|^2 + \frac{1}{2}|A|^4 \right) \mathrm{d}\xi, \tag{91}$$

where $\mathcal{F}$ plays the role of a free energy or Lyapunov functional. On examining the landscape of $\mathcal{F}$ one can see that stable time-independent spatially periodic solutions of (79) with different wavenumbers (81) must correspond to local minima of $\mathcal{F}$ and thus have basins of attraction separated by saddle-points of $\mathcal{F}$, which in turn occur at the points where the second variation of $\mathcal{F}$ is indefinite.

4.2.2 Time-Dependent Domain

Evidently, if the domain length L evolves on a timescale slower than the modulation timescale t in (79), then the above analysis for the time-independent domain applies, i.e., no differences are expected. Indeed, it does not matter whether (79) is analyzed in the original spatial variable x or after rescaling it via $x \to L\widehat{x}$—the results stay the same since the exponent

$$e^{ikx} = e^{i\widehat{k}\widehat{x}}, \quad \widehat{k} = Lk, \tag{92}$$

stays 'invariant' after such a transformation. If, on the other hand, the domain size evolves on the modulation timescale, $L = L(t)$, we may write $x \to L(t)x$ to eliminate the time-dependence of the domain, obtaining

$$\partial_t A = \mu A + \frac{1}{L^2(t)}\partial_x^2 A - |A|^2 A, \tag{93}$$

where x is now a Lagrangian (fixed domain) variable. This new form (93) of the GLE applies to translation-invariant systems as explained in [55], i.e., when the dilution and convection effects discussed in Sect. 3.1 are absent.

Equation (93) has elementary solutions of the form

$$A_Q(t,x) = a_Q(t)e^{iQx}, \tag{94}$$

where Q is time-independent and the amplitude $a_Q(t)$ can again be taken real and satisfies the equation

$$\dot{a}_Q = \left[\mu - \frac{Q^2}{L^2(t)}\right]a_Q - a_Q^3. \tag{95}$$

The solution (94) represents the base state in which the wavelength $2\pi L(t)/Q$ in the unscaled (Eulerian) variables is being stretched commensurably with the domain size. Note that base states of the form (94) with time-dependent $Q(t)$, i.e., with Eulerian wavelength $2\pi L(t)/Q(t)$ whose time-dependence differs from that of $L(t)$, do not exist. Perturbations (83) of the state (94) evolve according to

$$\frac{\mathrm{d}a_{k+}}{\mathrm{d}t} = \left[\mu - \frac{(Q+k)^2}{L^2(t)}\right]a_{k+} - a_Q^2(t)(2a_{k+} + a_{k-}), \tag{96a}$$

$$\frac{\mathrm{d}a_{k-}}{\mathrm{d}t} = \left[\mu - \frac{(Q-k)^2}{L^2(t)}\right]a_{k-} - a_Q^2(t)(2a_{k-} + a_{k+}). \tag{96b}$$

The key differences between these equations and (84a)–(84b) for the time-independent domain case are (a) the scaling of the perturbation wavenumbers $Q \pm k$ with the domain size $L(t)$, which destabilizes periodic states by shifting their wavenumber into the instability region, i.e., the domain size plays the role of a time-dependent bifurcation parameter, and (b) the time-dependent amplitude of the base state solution $a_Q(t)$ and hence the presence of the time-dependent factor a_Q^2 in the coupling of $a_{\pm k}$, which contributes to bifurcation delay.

In contrast to the time-independent domain case (84a)–(84b), the system (95), (96a)–(96b) is not amenable to spectral analysis. Other methods, such as energy and various types of estimates or inequality analysis, are therefore needed to obtain analytical insight (besides numerical investigation of sample problems). However, it should be mentioned that an alternative approach, based on a nonlinear diffusion equation for the phase ϕ, is also available [55]. In general, one can view the system (95), (96a)–(96b) either on short timescales, when transient phenomena such as bifurcation delays matter, or over long times that are necessary for understanding instabilities. For example, in the case $L(t) \to \text{const}$ as $t \to \infty$, one can perform a spectral analysis of (95), (96a)–(96b); more interesting cases correspond to either $L(t) \to \infty$ or $L(t) \to 0$ as $t \to \infty$—in the first case (stretching domain) one can easily show that the perturbation amplitude saturates at a constant value, while in the second case (shrinking domain) the base state will grow as $R(t) \sim t^\alpha$ for $L(t) \sim t^{-\alpha}$, $0 < \alpha < 1$, while the perturbation amplitude grows exponentially.

We can compute the bifurcation delay from the equations for the amplitude and phase of the solution $A(t,x) = R(t,x)e^{i\Phi(t,x)}$ of (93),

$$R_t = \mu R + \frac{1}{L^2(t)}\left(R_{xx} - R\Phi_x^2\right) - R^3, \tag{97a}$$

$$\Phi_t = \frac{1}{L^2(t)}\left(\Phi_{xx} + 2\frac{R_x\Phi_x}{R}\right), \tag{97b}$$

on the assumption that R and Φ evolve on the yet longer timescale $T = \epsilon^2 t \equiv \epsilon^4\widetilde{t}$ and on the yet larger spatial scale $X = \epsilon x \equiv \epsilon^2\widetilde{x}$, with $L(t)$ evolving on the timescale T as well [55]. In

particular, we examine the behavior of the perturbations $r(T, X)$, $\phi(T, X)$ of the base state $R = a_Q(t)$, $\Phi = Qx$:

$$A(t, x; T, X) = a_Q(t)\big[1 + \epsilon r(T, X)\big]e^{i(Qx+\phi(T,X))}. \tag{98}$$

To solve the equations for r, ϕ, we write $r = r_0 + \epsilon r_1 + \cdots$ and find that at leading order the r equation yields $r_0 = -Q\phi_X/L^2a_Q^2$—with this result the ϕ equation reduces to a time-dependent diffusion equation for the phase perturbation ϕ:

$$\phi_T = \frac{1}{L^2}\left(1 - \frac{2Q^2}{L^2a_Q^2}\right)\phi_{XX}, \tag{99}$$

where $a_Q^2(t) \equiv a_Q^2(T) = \mu - Q^2/L^2(T)$ as determined asymptotically from (95) on the long timescale T. Writing $\phi = \sum b_k(T)e^{ikX}$ we see that the amplitude b_k of a perturbation with wavenumber k satisfies

$$b_k' = -\frac{1}{L^2}\left(1 - \frac{2Q^2}{L^2a_Q^2}\right)k^2b_k = -\frac{1}{L^2}\left(\frac{\mu - \frac{3Q^2}{L^2}}{\mu - \frac{Q^2}{L^2}}\right)k^2b_k, \tag{100}$$

which is of the form (102) and thus exhibits bifurcation delay as described in the Appendix. In fact, one may compute the exact phase-slip delay compared to the time-independent domain case following the Appendix.

The above results imply that as the domain length L increases the instantaneous wavelength $2\pi L/Q$ of the periodic wavetrain will be pushed into the Eckhaus-unstable regime: at the Eckhaus instability the phase diffusion coefficient in (99) becomes negative. However, because of the bifurcation delay mentioned above the resulting phase slip will also be delayed, allowing the wavelength of the periodic state to stretch beyond that permitted by a time-independent analysis. A stationary state results when the delay becomes comparable to the stretching timescale—this is the condition that determines the wavenumber $Q(T)$ at which the phase slips can keep up with the changing wavelength.

To contrast the phase slip process in the time-dependent domain system (95), (96a)–(96b) with that in the time-independent domain case, one can also follow the *local* approach of [31] to show that the phase slip occurs at the time t^* defined by

$$\int_0^{t^*} \frac{\mathrm{d}\tau}{L^2(\tau)} = d, \tag{101}$$

provided that one starts from the same initial conditions as in (88) and looks for a solution in the form $A(t, x) = A_0(x) + f(t)$, implying that $f(t) = a\int_0^{t^*} L^{-2}(\tau)\mathrm{d}\tau$. As one can see from (101) by taking $L(t) = L(0) + l(t)$ with $l(t) = st^\alpha$, $\alpha > 0$, domain growth ($s > 0$) leads to a delay in the phase slip, while domain shrinkage ($s < 0$) brings the phase slip event closer compared to the time-independent domain case, $t^* = d$. Note that due to translation invariance of the system the phase slip can be supposed to take place at the origin, $x = 0$. The *global* problem for the time-dependent domain case remains open.

Extensions of the nonlinear theory of the Eckhaus instability [57, 62] to time-dependent domains is not straightforward as can be seen from the variational formulation (91) of (79). Namely, in the time-dependent domain case, the functional $\mathcal{F}$ becomes explicitly time-dependent and therefore the saddle-points of $\mathcal{F}$ are no longer stationary, which in turn makes the basins of attraction of solutions with different wavenumbers (number of cells)

time-dependent as well. The resulting difficulties are similar to those encountered in time-dependent perturbation theory in quantum mechanics and, more generally, in the theory of nonautonomous Hamiltonian theory discussed in Sect. 2.6.

5 Discussion: Key Challenges

The examples highlighted in this article point to the need for developing a set of theoretical tools necessary for understanding and quantifying various aspects of the rich dynamics exhibited in systems on time-dependent domains. Many of the key challenges center around pattern formation, and require one to understand both bifurcations and the mechanisms responsible for the formation and evolution of spatial structures. Advances in bifurcation theory should be able to tackle nonautonomous infinite-dimensional systems, where effects of both time-dependent domain size and time-dependent base state are present, as exemplified by the system (95), (96a)–(96b). Such a theory would allow one to determine the time-dependent saturated state resulting from dynamic bifurcation and delayed onset of instability. In addition to the dynamic character of the bifurcations brought about by the time-dependence of the domain size, the precise role of the conditions imposed on the boundaries requires further elucidation.

While certain progress in analyzing pattern formation on time-dependent domains has been made for translationally invariant systems [55], the *advection* and *dilution* effects discussed in Sect. 3 represent new challenges for understanding dynamics and instabilities in various systems, including those of reaction-diffusion type. Numerical simulations of stretching patterns in systems with propagating fronts and a preferred lengthscale reveal that, in addition to the delay in the phase slip generation, the phase slips have a preferred location [71] and do not take place uniformly throughout the pattern (in contrast to the example in Sect. 2.7). This location may or may not be in the center of the pattern, and may be selected by inhomogeneities in the amplitude of the pattern imposed by lateral boundary conditions. As observed in a number of examples, standard spectral analysis applicable to autonomous systems on time-fixed domains fails on time-dependent domains and therefore new approaches need to be developed, e.g. based on energy and other types of estimates to get bounds on the base state and perturbation growth. These would find wide applicability as can be seen from the variety of physical systems discussed in Sect. 2. And, of course, a good way to appreciate the universality of the instability phenomena in these different systems is to derive near-critical equations analogous to the Ginzburg-Landau equation in the time-independent domain case. These developments will contribute to the understanding of pattern formation in systems on time-dependent domains and, in particular, of the Eckhaus instability.

Besides these core questions pertinent to pattern formation, one may anticipate new questions dictated by the relevant physics, such as resonance phenomena that occur when the timescale of the domain deformation is comparable to the natural timescale of the problem at hand, or the effect of noise and inhomogeneities in triggering instabilities. For example, noise may affect both the location and timing of the Eckhaus instability because the instability is subcritical and the resulting super-exponential growth acts as a strong noise amplifier.

Acknowledgements This work was partially supported by the National Science Foundation (NSF) under Collaborative Research Grants CMMI-1232902 and CMMI-1233692, CAREER award under Grant No. 1054267, the Department of Defense DARPA Young Faculty Award Grant No. N66001-11-1-4130, and the Natural Sciences and Engineering Research Council of Canada (NSERC) under Grant No. 6186.

Appendix: Bifurcation Delay

Non-autonomous instability problems such as the ones described in Sect. 2 are often characterized by bifurcation delay phenomena. To understand the origin of this delay it is helpful [75] to consider a linear equation of nonautonomous type (2)

$$\frac{\mathrm{d}u}{\mathrm{d}t} = a(t)u, \qquad u(0) = u_0 > 0, \tag{102}$$

where a is a sufficiently smooth function, which changes sign at some '*turning point*' time $t_* > 0$ with $a(t) < 0$ on $t \in (0, t_*)$ and $a(t) > 0$ on $t \in (t_*, \infty)$. The solution to (102) shown in Fig. 14(a),

$$u(t) = u_0 \exp\left(\int_0^t a(s)\mathrm{d}s\right), \tag{103}$$

implies that an initial condition u_0 decays over the time interval $0 < t < t_*$ and then grows, so that at some time $t_{\mathrm{exit}} > t_*$ the exponent $\int_0^t a(t)\mathrm{d}t$ vanishes and for $t > t_{\mathrm{exit}}$ it grows. The time t_{exit}, defined by the equality $\int_0^{t_{\mathrm{exit}}} a(s)\mathrm{d}s = 0$, then implies that for $t > t_{\mathrm{exit}}$ the solution escapes (exits) from a ball of radius u_0 around $u = 0$ defined by the initial condition; the two times, t_{exit} and t_*, characterizing the instability onset, do not depend on the value of u_0. Because $t_{\mathrm{exit}} > t_*$, one usually speaks of a *bifurcation delay*. Hence the time at which the solution is repelled from the equilibrium $u = 0$ is given by t_{exit}, a time greater than t_* at which the equilibrium loses its stability should $a(t)$ be considered as a fixed (time-independent) parameter.

Note that while the growth is determined by the condition $\dot{u}(t) > 0$ leading to $a(t) > 0$ as follows from (103), this is not a necessary condition. Indeed, as can be seen from the case $a(t) = 1 + c\sin t$ with $|c| > 1$, the solution $u(t) = u(0)e^{t - c\cos t}$ grows despite the fact that $a(t)$ oscillates periodically between fixed positive and negative values.

A more interesting example of a bifurcation delay occurs in the context of a supercritical Hopf bifurcation [69, 87] described (in polar coordinates) by $\dot{\theta} = 1$, $\dot{u} = u[a(t) - u^2]$, $\dot{a} = \epsilon$ with $|\epsilon| \ll 1$, where the dynamics is infinitesimally slow with respect to the bifurcation parameter $a(t)$ from some initial negative value a_0 of $a(t)$ until it reaches a positive critical value at $t_{\mathrm{exit}} \simeq -a_0/\epsilon$ when the system abruptly begins to oscillate with a large amplitude, cf. Fig. 14(b).

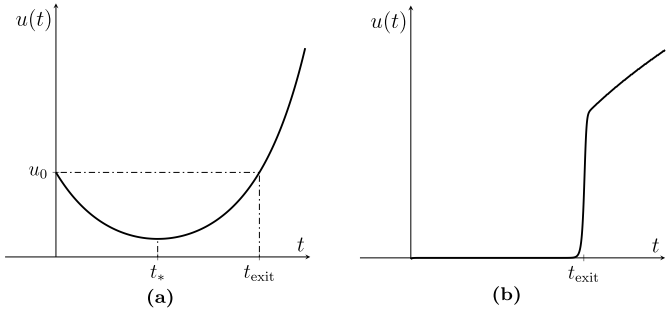

Fig. 14 Examples of bifurcation delay: (**a**) the solution (103) of (102) with $a(t) = t - 1$, (**b**) the Hopf bifurcation [69]

References

1. Ahlers, G., Cannell, D.S., Dominguez-Lerma, M.A., Heinrichs, R.: Wavenumber selection and Eckhaus instability in Couette-Taylor flow. Physica D **23**, 202–219 (1986)
2. Andresen, G.B., et al.: Autoresonant excitation of antiproton plasmas. Phys. Rev. Lett. **106**, 025002 (2011)
3. Angenent, S.: The zero set of a solution of a parabolic equation. J. Reine Angew. Math. **390**, 79–96 (1988)
4. Argentina, M., Mahadevan, L.: Fluid-flow-induced flutter of a flag. Proc. Natl. Acad. Sci. USA **102**, 1829–1834 (2005)
5. Armaou, A., Christofides, P.D.: Robust control of parabolic PDE systems with time-dependent spatial domains. Automatica **37**, 61–69 (2001)
6. Balazs, N.L.: On the solution of the wave equation with moving boundaries. J. Math. Anal. Appl. **3**, 472–484 (1961)
7. Ball, J.M.: Stability theory for an extensible beam. J. Differ. Equ. **14**, 399–418 (1973)
8. Bellman, R.: A survey of the theory of the boundedness, stability, and asymptotic behaviour of solutions of linear and nonlinear differential and difference equations. Tech. Rep. NAVEXOS P-596, Office of Naval Research, Washington DC (1949)
9. Billah, K.Y., Scanlan, R.H.: Resonance, Tacoma Narrows Bridge failure, and undergraduate physics textbooks. Am. J. Phys. **59**, 118–124 (1991)
10. Bisognin, E., Bisognin, V., Sepúlveda, M., Vera, O.: Coupled system of Korteweg-de Vries equations type in domains with moving boundaries. J. Comput. Appl. Math. **220**, 290–321 (2008)
11. Bisognin, V., Buriol, C., Ferreira, M.V., Sepúlveda, M., Vera, O.: Asymptotic behaviour for a nonlinear Schrödinger equation in domains with moving boundaries. Acta Appl. Math. **125**, 159–172 (2013)
12. Bock, D.N.: On the Navier-Stokes equations in noncylindribal domains. J. Differ. Equ. **25**, 151–162 (1977)
13. Burdzy, K., Chen, Z.Q., Sylvester, J.: The heat equation and reflected Brownian motion in time-dependent domains. II. Singularities of solutions. J. Funct. Anal. **204**, 1–34 (2003)
14. Burdzy, K., Chen, Z.Q., Sylvester, J.: The heat equation and reflected Brownian motion in time-dependent domains. Ann. Probab. **32**, 775–804 (2004)
15. Büttiker, M., Landauer, R.: Traversal time for tunneling. Phys. Rev. Lett. **49**, 1739–1742 (1982)
16. Cooper, J.: Asymptotic behavior for the vibrating string with a moving boundary. J. Math. Anal. Appl. **174**, 67–87 (1993)
17. Cooper, J., Koch, H.: The spectrum of a hyperbolic evolution operator. J. Funct. Anal. **133**, 301–328 (1995)
18. Craik, A.D.D.: The origins of water wave theory. Annu. Rev. Fluid Mech. **36**, 1–28 (2004)
19. Crampin, E.J., Gaffney, E.A., Maini, P.K.: Reaction and diffusion on growing domains: scenarios for robust pattern formation. Bull. Math. Biol. **61**, 1093–1120 (1999)
20. Crampin, E.J., Hackborn, W.W., Maini, P.K.: Pattern formation in reaction-diffusion models with nonuniform domain growth. Bull. Math. Biol. **64**, 747–769 (2002)
21. Crawford, J.D., Golubitsky, M., Gomes, M.G.M., Knobloch, E., Stewart, I.N.: Boundary conditions as symmetry constraints. In: Roberts, M., Stewart, I. (eds.) Singularity Theory and Its Applications. Lecture Notes in Mathematics, vol. 1463, pp. 63–79. Springer, Warwick (1989). Part II, New York (1991)
22. Cross, M.C., Hohenberg, P.C.: Pattern formation out of equilibrium. Rev. Mod. Phys. **65**, 851–1112 (1993)
23. da Costa, D.R., Dettmann, C.P., Leonel, E.D.: Escape of particles in a time-dependent potential well. Phys. Rev. E **83**, 066211 (2011)
24. Defay, R., Prigogine, I., Bellemans, A., Everett, D.: Surface Tension and Adsorption. Longmans Green and Co., London (1951)
25. Dembiński, S.T., Makowski, A.J., Peptowski, P.: Asymptotic behaviour of a particle in a uniformly expanding potential well. J. Phys. A, Math. Gen. **28**, 1449–1458 (1995)
26. Dickey, R.W.: Dynamic stability of equilibrium states of the extensible beam. Proc. Am. Math. Soc. **41**, 94–102 (1973)
27. Dittrich, J., Duclos, P., Šeba, P.: Instability in a classical periodically driven string. Phys. Rev. E **49**, 3535–3538 (1994)
28. Doescher, S.W., Rice, M.H.: Infinite square-well potential with a moving wall. Am. J. Phys. **37**, 1246–1249 (1969)
29. Drazin, P.G., Reid, W.H.: Hydrodynamic Stability. Cambridge University Press, Cambridge (2004)
30. Eckhaus, W.: Studies in Non-linear Stability Theory. Springer, New York (1965)

31. Eckmann, J.P., Gallay, T., Wayne, C.E.: Phase slips and the Eckhaus instability. Nonlinearity **8**, 943–961 (1995)
32. Fajans, J., Friedland, L.: Autoresonant (nonstationary) excitation of pendulums, Plutinos, plasmas, and other nonlinear oscillators. Am. J. Phys. **69**, 1096–1102 (2001)
33. Fajans, J., Gilson, E., Friedland, L.: Autoresonant (nonstationary) excitation of the diocotron mode in non-neutral plasmas. Phys. Rev. Lett. **82**, 4444–4447 (1999)
34. Fajans, J., Gilson, E., Friedland, L.: The effect of damping on autoresonant (nonstationary) excitation. Phys. Plasmas **8**, 423–427 (2001)
35. Feireisl, E., Nečasová, Š., Sun, Y.: Inviscid incompressible limits on expanding domains. Nonlinearity **27**, 2465–2477 (2014)
36. Fermi, E.: On the origin of the cosmic radiation. Phys. Rev. **75**, 1169–1174 (1949)
37. Fernández, M.A., Tallec, P.L.: Linear stability analysis in fluid-structure interaction with transpiration. Part I: Formulation and mathematical analysis. Comput. Methods Appl. Mech. Eng. **192**, 4805–4835 (2003)
38. Ferreira, J., Benabidallah, R., Muñoz Rivera, J.E.: Asymptotic behaviour for the nonlinear beam equation in a time-dependent domain. Rend. Mat. Appl. **19**, 177–193 (1999)
39. Filo, J., Zaušková, A.: 2D Navier-Stokes equations in a time dependent domain with Neumann type boundary conditions. J. Math. Fluid Mech. **12**, 1–46 (2010)
40. Fokas, A.S., Pelloni, B.: Integrable evolution equations in time-dependent domains. Inverse Problems **17**, 919–935 (2001)
41. Fortuin, L.: The wave equation in a medium with a time-dependent boundary. J. Acoust. Soc. Am. **53**, 1683–1685 (1973)
42. Frenk, C.S.: The origin of cosmic structure. In: Ellis, N. (ed.) 2nd CERN-CLAF School of High-Energy Physics, Geneva, CERN, pp. 239–259 (2006)
43. Garcia R., C., Minzoni, A.A.: An asymptotic solution for the wave equation in a time-dependent domain. SIAM Rev. **23**, 1–9 (1981)
44. Gonzalez, N.: An example of pure stability for the wave equation with moving boundary. J. Math. Anal. Appl. **228**, 51–59 (1998)
45. Green, A.E., Naghdi, P.M.: A derivation of equations for wave propagation in water of variable depth. J. Fluid Mech. **78**, 237–246 (1976)
46. Hartong-Redden, R., Krechetnikov, R.: Pattern identification in systems with S(1) symmetry. Phys. Rev. E **84**, 056212 (2011)
47. Hayes, B.: A box of Universe. Am. Sci. **100**, 10–15 (2012)
48. He, C., Hsiao, L.: Two-dimensional Euler equations in a time dependent domain. J. Differ. Equ. **163**, 265–291 (2000)
49. Holmes, M.H.: Introduction to the Foundations of Applied Mathematics. Springer, Berlin (2009)
50. Jeans, J.H.: The stability of a spherical nebula. Philos. Trans. R. Soc. Lond. A **199**, 1–53 (1902)
51. Kamke, E.: Handbook of Ordinary Differential Equations. Fizmatgiz, Moscow (1961)
52. Kaya-Cekin, E., Aulisa, E., Ibragimov, A., Seshaiyer, P.: Fluid structure interaction problem with changing thickness non-linear beam. Discrete Contin. Dyn. Syst. **Suppl.**, 813–823 (2011)
53. Kirr, E., Weinstein, M.I.: Parametrically excited Hamiltonian partial differential equations. SIAM J. Math. Anal. **33**, 16–52 (2001)
54. Knobloch, E.: On the decay of cosmic turbulence. Astrophys. J. **221**, 395–398 (1978)
55. Knobloch, E., Krechetnikov, R.: Stability on time-dependent domains. J. Nonlinear Sci. **24**, 493–523 (2014)
56. Kramer, L., Hohenberg, P.C.: Effects of boundary conditions on spatially periodic states. Physica D **13**, 357–369 (1984)
57. Kramer, L., Zimmermann, W.: On the Eckhaus instability for spatially periodic patterns. Physica D **16**, 221–232 (1985)
58. Krechetnikov, R.: A linear stability theory on time-invariant and time-dependent spatial domains with symmetry: the drop splash problem. Dyn. Partial Differ. Equ. **8**, 47–67 (2011)
59. Krechetnikov, R., Homsy, G.M.: Crown-forming instability phenomena in the drop splash problem. J. Colloid Interface Sci. **331**, 555–559 (2009)
60. Landau, L.D., Lifschitz, E.M.: Quantum Mechanics: Non-relativistic Theory. Butterworth, Stoneham (1976)
61. Langer, J.S.: Instabilities and pattern formation in crystal growth. Rev. Mod. Phys. **52**, 1–28 (1980)
62. Langer, J.S., Ambegaokar, V.: Intrinsic resistive transition in narrow superconducting channels. Phys. Rev. **164**, 498–510 (1967)
63. Lee, K.: A mixed problem for hyperbolic equations with time-dependent domain. J. Math. Anal. Appl. **16**, 471–495 (1966)

64. Leonel, E.D., Kamphorst Leal da Silva, J.: Dynamical properties of a particle in a classical time-dependent potential well. Physica A **323**, 181–196 (2003)
65. Leonel, E.D., McClintock, P.V.E.: Scaling properties for a classical particle in a time-dependent potential well. Chaos **15**, 033701 (2005)
66. Lewis, H.R. Jr.: Classical and quantum systems with time-dependent harmonic-oscillator-type Hamiltonians. Phys. Rev. Lett. **18**, 510–512 (1967)
67. Lichtenberg, A., Lieberman, M.: Regular and Chaotic Dynamics. Springer, Berlin (1992)
68. Lions, P.L., Sznitman, A.S.: Stochastic differential equations with reflecting boundary conditions. Commun. Pure Appl. Math. **37**, 511–537 (1984)
69. Lobry, C.: Dynamic bifurcations. In: Dynamic Bifurcations, pp. 1–13. Springer, Berlin (1991)
70. Lopes, O.: On the structure of the spectrum of a linear time periodic linear wave equation. J. Anal. Math. **47**, 55–68 (1986)
71. Ma, Y.P., Knobloch, E.: Depinning, front motion, and phase slips. Chaos **22**, 033101 (2012)
72. Mackenzie, J.A., Madzvamuse, A.: Analysis of stability and convergence of finite-difference methods for a reactiondiffusion problem on a one-dimensional growing domain. IMA J. Numer. Anal. **31**, 212–232 (2011)
73. Madzvamuse, A.: Turing instability conditions for growing domains with divergence free mesh velocity. Nonlinear Anal. **71**, e2250–e2257 (2009)
74. Madzvamuse, A., Gaffney, E.A., Maini, P.K.: Stability analysis of non-autonomous reaction-diffusion systems: the effects of growing domains. J. Math. Biol. **61**, 133–164 (2010)
75. Maesschalck, P.D., Popovic, N., Kaper, T.J.: Canards and bifurcation delays of spatially homogeneous and inhomogeneous types in reaction-diffusion equations. Adv. Differ. Equ. **14**, 943–962 (2009)
76. Maier, R.S., Stein, D.L.: Noise-activated escape from a sloshing potential well. Phys. Rev. Lett. **86**, 3942 (2001)
77. Makowski, A.J., Dembiński, S.T.: Exactly solvable models with time-dependent boundary conditions. Phys. Lett. A **154**, 217–220 (1991)
78. Makowski, A.J., Pepiowski, P.: On the behaviour of quantum systems with time-dependent boundary conditions. Phys. Lett. A **163**, 142–151 (1992)
79. Miyakawa, T., Teramoto, Y.: Existence and periodicity of weak solutions of the Navier-Stokes equations in a time dependent domain. Hiroshima Math. J. **12**, 513–528 (1982)
80. Miyashita, S.: Conveyance of quantum particles by a moving potential well. J. Phys. Soc. Jpn. **76**, 104003 (2007)
81. Modi, V.J., Ibrahim, A.M.: Vibration/libration interaction dynamics during the orbiter-based deployment of flexible members. In: Proceedings of the Workshop on Identification and Control of Flexible Structures. Jet Propulsion Laboratory, Pasadena (1985)
82. Morales, D.A., Parra, Z., Almeida, R.: On the solution of the Schrödinger equation with time dependent boundary conditions. Phys. Lett. A **185**, 273–276 (1994)
83. Munier, A., Burgan, J.R., Feix, M., Fijalkow, E.: Schrödinger equation with time-dependent boundary conditions. J. Math. Phys. **22**, 1219–1223 (1981)
84. Murray, J.D.: Mathematical Biology: I. An Introduction. Springer, Berlin (2007)
85. Naaman, O., Aumentado, J., Friedland, L., Wurtele, J.S., Siddiqi, I.: Phase-locking transition in a chirped superconducting Josephson resonator. Phys. Rev. Lett. **101**, 117005 (2008)
86. Neishtadt, A., Vasiliev, A.: Capture into resonance in dynamics of a classical hydrogen atom in an oscillating electric field. Phys. Rev. E **71**, 056623 (2005)
87. Neishtadt, A.I.: On stability loss delay for dynamical bifurcations. Discrete Contin. Dyn. Syst., Ser. S, **2**, 897–909 (2009)
88. Neville, A.A., Matthews, P.C., Byrne, H.M.: Interactions between pattern formation and domain growth. Bull. Math. Biol. **68**, 1975–2003 (2006)
89. Ng, J., Dubljevic, S.: Optimal control of transport-reaction system with time varying spatial domain. In: Kothare, M., Tade, M., Wouwer, A.V., Smets, I. (eds.) Proceedings of the 9th International Symposium on Dynamics and Control of Process Systems, Leuven, Belgium, pp. 587–592 (2010)
90. Ogawa, N., Furukawa, Y.: Surface instability of icicles. Phys. Rev. E **66**, 041202 (2002)
91. Painter, K.J., Maini, P.K., Othmer, H.G.: Stripe formation in juvenile Pomacanthus explained by a generalized turing mechanism with chemotaxis. Proc. Natl. Acad. Sci. USA **96**, 5549–5554 (1999)
92. Park, Y., Do, Y., Lopez, J.M.: Slow passage through resonance. Phys. Rev. E **84**, 056604 (2011)
93. Paul, W.: Electromagnetic traps for charged and neutral particles. Rev. Mod. Phys. **62**, 531–540 (1990)
94. Peebles, P.J.E.: Large-Scale Structure of the Universe. Princeton University Press, Princeton (1980)
95. Petrovskii, I.G.: On the solution of the first boundary value problem for the heat equation. Uch. Zap. Moskov. Gos. Univ. **2**, 55–59 (1934)
96. Pinder, D.N.: The contracting square quantum well. Am. J. Phys. **58**, 54–58 (1990)

97. Plaza, R.G., Sánchez-Garduño, F., Padilla, P., Barrio, R.A., Maini, P.K.: The effect of growth and curvature on pattern formation. J. Dyn. Differ. Equ. **16**, 1093–1121 (2004)
98. Plesset, M.S.: On the stability of fluid flows with spherical symmetry. J. Appl. Phys. **25**, 96–98 (1954)
99. Reimann, P., Evstigneev, M.: Pulsating potential ratchet. Europhys. Lett. **78**, 50004 (2007)
100. Richard, J., Nicoud, F.: Effect of the fluid structure interaction on the aeroacoustic instabilities of solid rocket motors. In: 32nd AIAA Aeroacoustics Conference on 17th AIAA/CEAS Aeroacoustics Conference, Portland, Oregon, pp. 1–15 (2011)
101. Rogak, E.D.: A mixed problem for the wave equation in a time dependent domain. Arch. Ration. Mech. Anal. **22**, 24–36 (1966)
102. Saffman, P.G., Taylor, G.: The penetration of a fluid into a medium or Hele-Shaw cell containing a more viscous liquid. Proc. R. Soc. Lond. Ser. A **245**, 312–329 (1958)
103. Schiff, L.I.: Quantum Mechanics. McGraw-Hill, New York (1949)
104. Scriven, L.E.: Dynamics of a fluid interface. Chem. Eng. Sci. **12**, 98–108 (1960)
105. Shelley, M.J., Tiany, F.R., Wlodarski, K.: Hele-Shaw flow and pattern formation in a time-dependent gap. Nonlinearity **10**, 1471–1495 (1997)
106. Sikorav, J.: A linear wave equation in a time dependent domain. J. Math. Anal. Appl. **153**, 533–548 (1990)
107. Skorokhod, A.V.: Stochastic equations for diflusion processes in a bounded region. Teor. Veroâtn. Ee Primen. **6**, 264–274 (1961)
108. Soffer, A., Weinstein, M.I.: Nonautonomous Hamiltonians. J. Stat. Phys. **93**, 359–391 (1998)
109. Stefan, J.: Über die Theorie der Eisbildung, insbesondere über die Eisbildung im Polarmeere. Ann. Phys. Chem. **42**, 269–286 (1891)
110. Stone, H.A.: A simple derivation of the time-dependent convective-diffusion equation for surfactant transport along a deforming interface. Phys. Fluids A **2**, 111–112 (1990)
111. Teramoto, Y.: On the stability of periodic solutions of the Navier-Stokes equations in a noncylindrical domain. Hiroshima Math. J. **13**, 607–625 (1983)
112. Theodorsen, T.: General theory of aerodynamic instability and the mechanism of flutter. Tech. Rep. 496, NACA (1949)
113. Tuckerman, L.S., Barkley, D.: Bifurcation analysis of the Eckhaus instability. Physica D **46**, 57–86 (1990)
114. Turing, A.M.: The chemical basis of morphogenesis. Philos. Trans. R. Soc. Lond. B **237**, 37–72 (1952)
115. Ueda, H.: A remark on parametric resonance for wave equations with a time periodic coefficient. Proc. Jpn. Acad., Ser. A, Math. Sci. **87**, 128–129 (2011)
116. Ueda, K.I., Nishiura, Y.: A mathematical mechanism for instabilities in stripe formation on growing domains. Physica D **241**, 37–59 (2012)
117. Vanneste, J., Wirosoetisno, D.: Two-dimensional Euler flows in slowly deforming domains. Physica D **237**, 774–799 (2008)
118. Vladimirov, V.S.: Equations of Mathematical Physics. Mir, Moscow (1984)
119. Volpert, V., Petrovskii, S.: Reaction-diffusion waves in biology. Phys. Life Rev. **6**, 267–310 (2009)
120. Vuik, C.: Some historical notes about the Stefan problem. Nieuw Arch. Wiskd. **11**, 157–167 (1993)
121. Wang, P.K.C.: Stabilization and control of distributed systems with time-dependent spatial domains. J. Optim. Theory Appl. **65**, 331–362 (1990)